

GAD- and GABA-Immunoreactivity in the Ascending Auditory Pathway of Horseshoe and Mustached Bats

MARIANNE VATER, MANFRED KÖSSL, AND ANJA K.E. HORN

Zoologisches Institut, (M.V., M.K.), Institut für Neuropathologie, LMU (A.K.E.H.), 8 München 2, Germany

ABSTRACT

A comparative study of the immunostain to antibodies directed against glutamic acid decarboxylase (GAD) and gamma-aminobutyric acid (GABA) in the ascending auditory pathway was carried out in horseshoe bats (*Rhinolophus rouxi*) and mustached bats (*Pteronotus parnellii*).

In both species GAD/GABA-positive puncta (presumed axonal boutons) and GAD/GABA-positive cells were found in the cochlear nucleus, the superior olivary complex, the nuclei of the lateral lemniscus, the inferior colliculus, and the medial geniculate body. General features of the immunostaining pattern in the auditory pathway agree with observations in other mammals. Quantitative analysis of puncta distribution shows that many auditory centers are characterized by subregional differences in puncta density and distribution. This indicates local differences in putatively inhibitory input related to connectivity and tonotopic organization.

The following species characteristic features were found: 1) The dorsal non-laminated portion of the dorsal cochlear nucleus in horseshoe bats lacks the GAD/GABA-immunoreactive cells typical for the ventral laminated portion and the dorsal cochlear nucleus of other species. Clearly, a cytoarchitectonic specialization is accompanied by a loss of putatively GABAergic local inhibitory circuits. 2) The ventral division of the medial geniculate body of the mustached bat lacks GAD/GABA-immunopositive cells. Such cells are present in the horseshoe bat and other mammals. This finding implies functional differences in the organization of the medial geniculate body within the same mammalian order. © 1992 Wiley-Liss, Inc.

Key words: auditory system, inhibition, neurotransmitters, immunocytochemistry

Immunohistochemical staining techniques with antibodies directed against specific neurotransmitters or their synthesizing enzymes have enhanced knowledge of the functional organization of the ascending auditory system of mammals. In particular, the inhibitory neurotransmitter gamma-aminobutyric acid (GABA) is known to play an important role in auditory processing. All nuclei of the auditory brainstem contain neuronal elements positively staining for antibodies directed against GABA or its synthesizing enzyme, glutamic acid decarboxylase (GAD; e.g., Adams and Mugnaini, '84; Mugnaini, '85; Thompson et al., '85; Peyret et al., '86; Wenthold et al., '86; Moore and Moore, '87; Roberts and Ribak, '87; Winer and Larue, '88; Saint-Marie et al., '89a; Adams and Mugnaini, '90; Caspary et al., '90). These studies demonstrate that the distribution of immunolabeled cells and boutons is characteristic for a particular auditory center and forms the substrate for intrinsic inhibitory circuits as well as ascending and descending inhibitory projections. Physiological studies have revealed that GABA-mediated inhibition serves a variety of

functions at different integration levels. For instance, GABA is known to influence spike-count functions of single cochlear nucleus cells (Caspary, '86; Caspary et al., '79), to mediate tone-evoked monaural and binaural inhibition in cells of the inferior colliculus (e.g., Faingold et al., '89), and to increase neuronal selectivity for complex acoustic stimuli in the avian auditory forebrain (Müller and Scheich, '87).

This paper describes the distribution of GAD- and GABA-immunoreactivity within the auditory brainstem centers and the medial geniculate body (MGB) of two echolocating bats: the horseshoe bat (*Rhinolophus rouxi*) and the mustached bat (*Pteronotus parnellii*). These species are classified as CF-FM bats (CF refers to the long constant frequency call component, FM to the frequency modulated component) and have independently evolved a Doppler-

Accepted June 9, 1992.

M. Vater's present address is Zoologisches Institut, Universitätsstr. 31, 84 Regensburg, Germany.

sensitive sonar system (review: Schnitzler and Henson, '80). Their most striking common feature in auditory processing is the cochlear and central overrepresentation of a narrow frequency band encompassing the species characteristic second harmonic CF-signal frequency, which is 78 kHz in the horseshoe bat and 60 kHz in the mustached bat (review: Pollak and Casseday, '89). Apart from this basic similarity, a number of species characteristic features in the cytoarchitecture of auditory centers and their tonotopic arrangements have been demonstrated (e.g., Schweizer, '81; Zook and Casseday, '82a,b; Zook et al., '85; Feng and Vater, '85; Ross et al., '88; Kössl and Vater, '90; Vater and Feng, '90). Since the functional role of inhibition in monaural and binaural auditory processing in the auditory brainstem has been investigated in numerous physiological studies of these species (e.g., Neuweiler and Vater, '77; Schlegel, '77; Möller, '78; Wenstrup et al., '86; review: Pollak and Casseday, '89), they offer a good opportunity for correlating immunocytochemical results with functional aspects. The goal of the present study was to provide maps of the neuronal substrate for GABA-mediated inhibitory interactions in the auditory system of these two non-related CF-FM bats, with particular emphasis on the question whether species characteristic features of the functional organization of the ascending auditory pathway are also expressed in the organization of the transmitter profiles. Furthermore, we provide details on GAD/GABA-immunopositive cell types and the relative amount of putatively GABAergic innervation of auditory centers which can be compared with data from less specialized mammals.

MATERIALS AND METHODS

The brains of five adult horseshoe bats and four adult mustached bats were used. Six brains were processed for GAD-immunocytochemistry according to the protocol of Oertel et al. ('81) and three brains (two horseshoe bats, one mustached bat) were prepared for GABA-immunocytochemistry. Under deep nembutal anaesthesia (25 mg/100 g), the bats were perfused through the heart with normal saline followed by a fixative containing 4% paraformaldehyde in 0.1 M phosphate buffer (pH 7.4) for the GAD-immunocytochemistry or a fixative consisting of 1–2% paraformaldehyde and 0.5–1% glutaraldehyde in 0.1 M phosphate buffer

for GABA-immunocytochemistry. The brains were removed from the skull and postfixed for 1–2 hours in the respective fixatives prior to cutting sections of 25 or 50 μ m thickness with a vibratome (Oxford). Eight brains were cut in the frontal plane and one brain (mustached bat; GAD-immunocytochemistry) in the sagittal plane. One series of alternating sections was directly mounted on glass slides and stained with cresylviolet for assessment of cytoarchitecture. The other series was processed as free-floating sections for GAD- and GABA-immunocytochemistry following the peroxidase-antiperoxidase (PAP)-method (Sternberger, '79) or Avidin-Biotin-method (Hsu et al., '81). The GAD-antibody (sheep) was kindly supplied by W.H. Oertel and was used at a dilution of 1:2,000, the GABA-antibody (INCSTAR; rabbit) was diluted to 1:4,000 or 1:5,000. Sections were thoroughly washed in phosphate buffered saline (3×10 minutes) and endogenous peroxidases were inactivated by treating the sections in 10% methanol/3% H_2O_2 prior to preincubation (1 hour) with normal goat serum (GABA) or normal rabbit serum (GAD) for 1 hour, followed by an overnight incubation with the primary antibody. For control sections, the primary antibody was omitted. The PAP and avidin-biotin complexes were visualized by treating the sections with 0.05% diaminobenzidine and 0.01% peroxide for 10–15 minutes. Sections were thoroughly rinsed in buffer, mounted on gelatine coated slides and coverslipped with Depex mounting medium.

Sections were analyzed with the light microscope at magnifications from $\times 40$ to $\times 1,250$. A stained cell was classified as immunopositive for GAD if the cytoplasm contained brown reaction product and was clearly distinct from the unstained nucleus. Lightly stained cells were not considered immunoreactive. GABA-positive cells were characterized by brown cytoplasmic staining, dark brown staining of the nucleus and an unstained nucleolus. Stain intensity was found to differ among cells in different auditory centers. Therefore immunoreactive cells were classified as either moderately or darkly stained with reference to stain intensity of cells in the inferior colliculus or the dorsal nucleus of the lateral lemniscus (DNLL) which were most darkly stained. Stained neuronal elements further included punctiform profiles in the neuropil, in close contact to stained or unstained somata or proximal dendrites. Puncta presumably representing immunopositive

Abbreviations

a	anterior	ICc	central nucleus of the inferior colliculus
al	anterolateral	ICx	external nucleus of the inferior colliculus
AN	auditory nerve	INLL	intermediate nucleus of the lateral lemniscus
AVCN	anteroventral cochlear nucleus	INT	interstitial nucleus
c	central	l	lateral
Cer	cerebellum	LNTB	lateral nucleus of the trapezoid body
CF	constant frequency	LL	lateral lemniscus
CN	cochlear nucleus	LSO	lateral superior olivary nucleus
d	dorsal	m	medial
dd	dorsal region of PVCNd	ma	marginal cell group of the CN
dp	dorsoposterior	MGB	medial geniculate body
dv	ventral region of PVCNd	MSO	medial superior olivary nucleus
DAB	Diaminobenzidine	MNTB	medial nucleus of the trapezoid body
DCN	dorsal cochlear nucleus	NOC	nucleus olivocochlearis
DMSO	dorsomedial superior olive	PLZ	paralemniscal zone
DMPO	dorsomedial periolivary nucleus	PVCN	posteroventral cochlear nucleus
DNLL	dorsal nucleus of the lateral lemniscus	SOC	superior olivary complex
FM	frequency modulated	v	ventral
GABA	gamma-aminobutyric acid	vm	ventromedial
GAD	glutamic acid decarboxylase	VMSO	ventral medial superior olivary nucleus
HRP	horseradish peroxidase	VNLL	ventral nucleus of the lateral lemniscus
IC	inferior colliculus	VNTB	ventral nucleus of the trapezoid body

axonal terminals were distinguished from cut fiber or dendritic profiles by their characteristic shape and distribution. In general, the distribution of stained neuronal elements was similar with both antibodies; however the staining of puncta profiles was more prominent with the GAD-antibody, whereas the staining of cells was more prominent with the GABA-antibody. GAD-immunocytochemistry was used to assess quantitatively the distribution of labeled puncta. In cases where prominent puncta staining with the GAD-antibody severely masked the labeled cells (e.g., outer fusiform cell layer of the DCN, periolivary cell groups), the cell types were analysed from GABA-immunostained material.

For quantitative analysis, cell size was measured with a minimop (Kontron) and is given as somatic area in square micrometers. Only those cells with clearly visible nucleus were measured. Puncta (i.e., presumed axon terminals) were observed at $\times 1,000$ to $\times 1,250$ magnification. In order to define relative regional variations in puncta density within auditory centers, puncta were counted in drawings of a defined area of $1,000 \mu\text{m}^2$ made in one focal plane of the section. For each cytoarchitectonic area at least ten positions were analysed. Only those puncta were included in the analysis which fulfilled the following criteria (see also Winer and Larue, '88): they must be confined to the focal plane of the section; they must not show signs of continuity through the depth of the section. Immunostained dendritic profiles were omitted from the analysis.

Specificity of label: For the following reasons we conclude that the staining pattern in the auditory system of bats is specific: 1) Control experiments in which the primary antiserum was omitted did not yield staining. 2) The pattern seen is in general accordance with reports on the auditory system of other mammals. 3) Both GABA- and GAD-antibodies were tested and yielded basically similar results. Since we did not use colchicine-treatment (e.g., Mugnaini, '85), staining of cells with the GAD-antibody appeared to be less prominent than with the GABA-antibody.

RESULTS

Previous studies have described the cytoarchitecture of the brainstem auditory centers in the horseshoe bat (Schweizer, '81; Feng and Vater, '85; Casseday et al., '88; Vater and Feng, '90) and the mustached bat (Zook and Casseday, '82a, Zook et al., '85). The basic organization of the ascending auditory pathway in the two bats is similar to that in other mammals, each species, however, has characteristic specializations. In order to point out species-characteristic organizational features of auditory nuclei, as well as the differential distribution of immunostained neuronal elements, the GAD/GABA-labeling pattern in the main stations of the ascending auditory pathway up to the diencephalic level is shown in Figure 1 for both bats (circles denote stained cells, stippling denotes stained puncta). We will refer to this map in later detailed descriptions of individual auditory centers. Briefly, as in other mammals, the cochlear nucleus (CN) is composed of three subdivisions (anteroventral, posteroventral and dorsal, i.e., AVCN, PVCN, DCN). In the horseshoe bat, a prominent feature is the presence of a non-laminated dorsal portion of the DCN (DCNd), in addition to a ventral laminated portion (DCNv) (Feng and Vater, '85). In the mustached bat the DCN is laminated throughout its extent (Zook and Casseday, '82a).

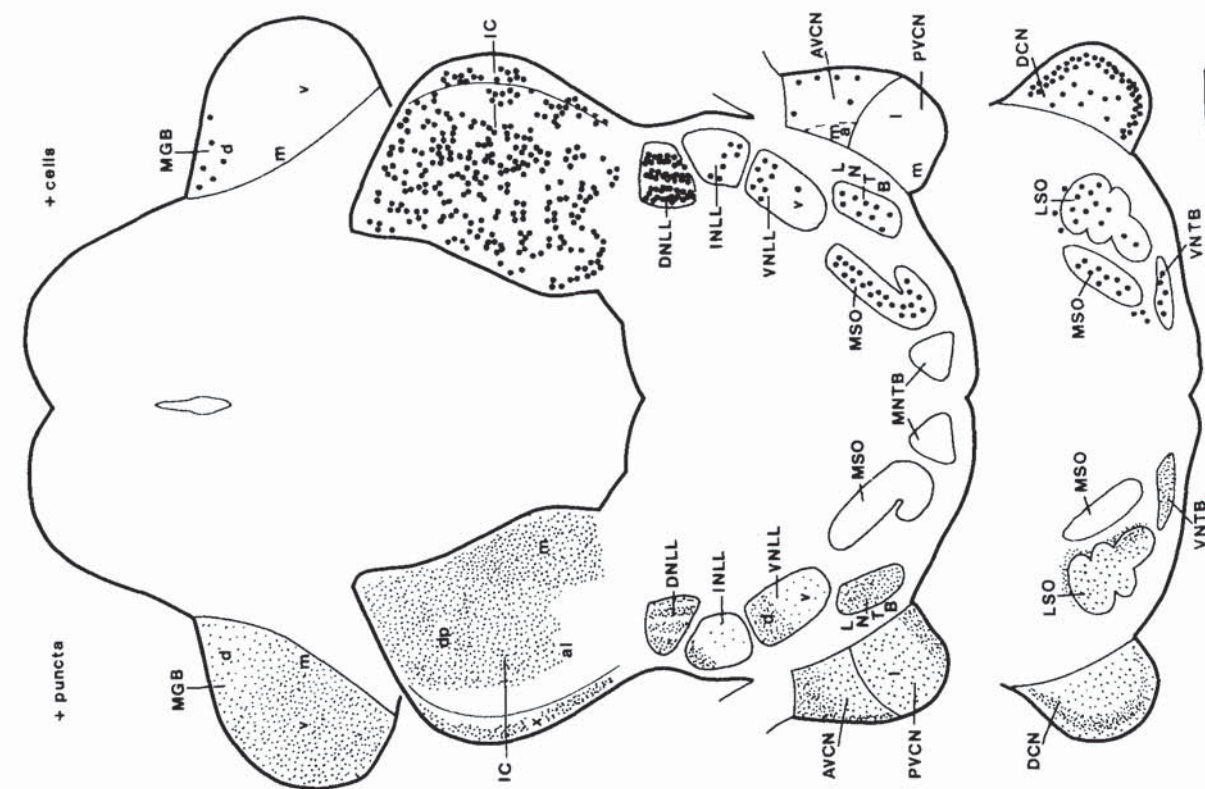
A specialized feature of the mustached bat is the marginal cell group of the medial AVCN (ma, Zook and Casseday, '82a; Kössl et al., '88). The superior olivary complex (SOC) of the mustached bat is composed of three principal nuclei, the lateral superior olive (LSO), the medial superior olive (MSO), and the medial nucleus of the trapezoid body (MNTB) (Zook and Casseday, '82a). These are surrounded by periolivary structures (ventral and lateral nucleus of the trapezoid body; VNTB, LNTB). In the horseshoe bat, the organization of the nuclear groups located between the LSO and MNTB deviates from other species. There are two distinct nuclei, the dorsal medial superior olive (DMSO) and the ventral medial superior olive (VMSO), respectively, which are not clearly comparable with the MSO (Casseday et al., '88; Vater and Feng, '90). In both species, the nuclei of the lateral lemniscus (LL) are hypertrophied and distinctly organized into a dorsal nucleus (DNLL), an intermediate nucleus (INLL), and a ventral nucleus (VNLL) (Schweizer, '81; Zook and Casseday, '82a). The VNLL is further subdivided into a dorsal (d) and ventral part (v) in the mustached bat and into a lateral (l) and medial (m) part in the horseshoe bat. In the horseshoe bat a paralemniscal zone (PLZ) is continuous with the DNLL (Metzner, '89). The main midbrain auditory center, the inferior colliculus (IC), is highly developed in both species and can be subdivided into the central nucleus (ICc) and the external nucleus (ICx). For the purpose of the present study, the ICc of the horseshoe bat will be partitioned into dorsal (d), ventral (v) and ventromedial (vm) regions. According to Zook et al. ('85) the ICc of the mustached bat is divided into the anterolateral division (al), the dorsoposterior division (dp), and the medial division (m). The medial geniculate body (MGB) is a prominent diencephalic auditory integration center, but details on its cytoarchitectonic subdivisions have not been published. In this study it will be grossly subdivided into a dorsal, medial and ventral division. In the following, the characteristic distribution of immunostaining in each auditory center will be described in detail.

Cochlear nucleus

Each subdivision of the cochlear nucleus is characterized by a typical morphology and distribution of immunostained neuronal elements. Additionally, there are subregional differentiations within the subdivisions.

AVCN. The labeling pattern in the AVCN of the horseshoe bat is illustrated in Figures 2A and 3. GAD/GABA-positive puncta were found throughout the AVCN. Puncta density was especially high in the granular cell cap of the AVCN, which surrounds its dorsal and lateral margin (Fig. 2A). The central region of the AVCN contained fewer puncta per unit area than the dorsal and lateral regions (Fig. 3, bar diagram). This feature correlates both with cell packing density which is lower in central regions than in the other zones and with absolute numbers of puncta per neuron. In central regions of the AVCN, 8–12 GAD-positive puncta formed perisomatic rings and clusters on non-stained spherical cell bodies (Fig. 2B). In dorsal and lateral regions of the AVCN, 12–20 puncta formed distinct perisomatic rings on non-stained cell bodies. Furthermore, in dorsal and lateral regions puncta size tended to be larger (mean longest diameter $2 \mu\text{m}$, range $1.2 \mu\text{m}$ – $3 \mu\text{m}$) than in central regions (mean $1.4 \mu\text{m}$, range $0.9 \mu\text{m}$ – $2.4 \mu\text{m}$). Only few immunopositive cell bodies were scattered in the central parts and along the lateral and medial margins (Fig. 3). Their somata were oval and mainly of intermediate size

Pteronotus



Rhinolophus

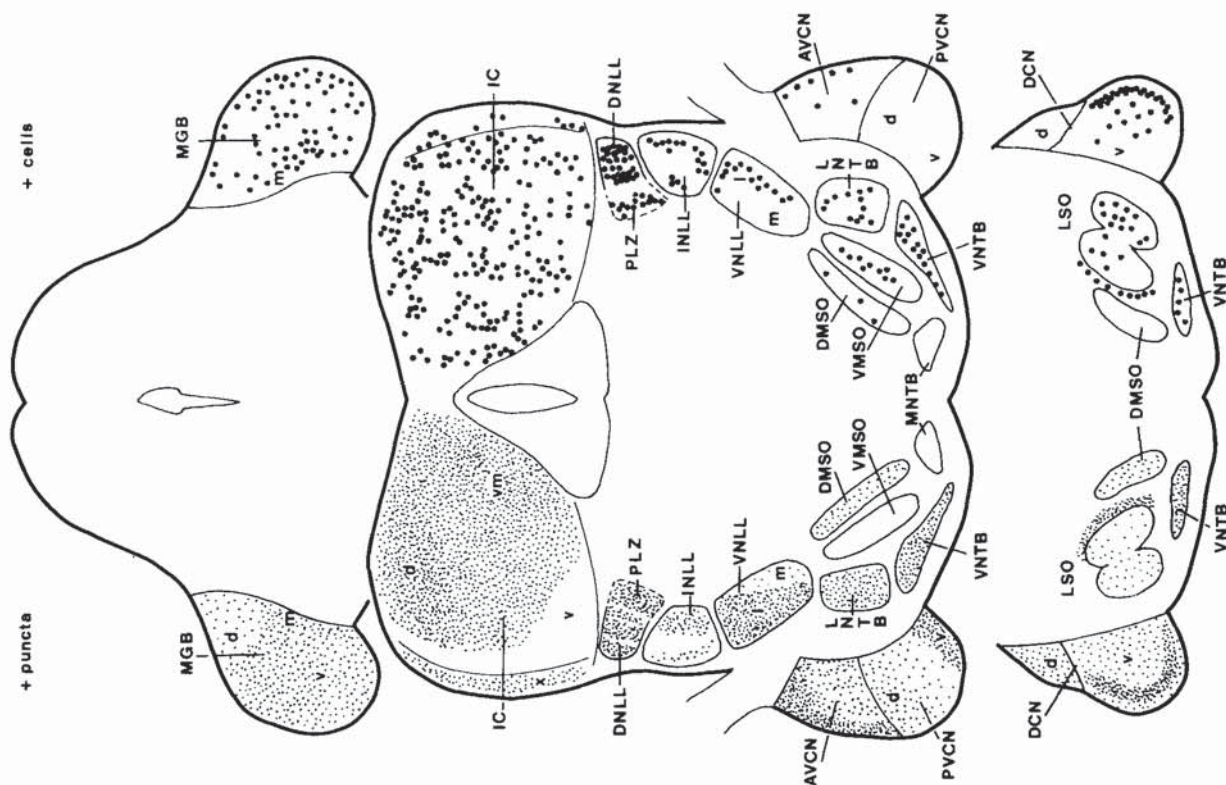


Figure 1

(mean area $70.5 \mu\text{m}^2$, range $35\text{--}93 \mu\text{m}^2$). These cells generally received fewer puncta (1–6) than non-labeled cell bodies. Similar labeling patterns were observed in the mustached bat. Puncta density in the anterior division of the AVCN was distinctly higher than in the posterior division of the AVCN (Fig. 3, bar diagram). The marginal cell area (ma) of the AVCN which preferentially responds to the frequency range of the first harmonic FM-component (Kössl and Vater, '90) did not contain labeled somata and the unlabeled cell bodies were encircled by fewer puncta than cells in the central region of the AVCN.

PVCN. No immunostained somata were observed in the PVCN of the horseshoe bat (Figs. 2A, 3). There were clear differences in the puncta supply of the dorsal subregion (PVCNd), which represents the CF- and FM-components of the echolocation signal (Feng and Vater, '85) and the ventral subregion (PVCNv), which represents the lower frequency range (Figs. 2A, 3, bar diagram). The density of stained puncta per unit area and per non-stained cell is highest in the PVCNv, where the somata and proximal dendrites of multipolar neurons are densely studded with GAD-positive puncta (Fig. 2C). There are relatively few puncta in the PVCNd. These either formed perisomatic rings on round cell bodies or were preferentially distributed on the origin of and along the dendritic profiles of large bipolar or multipolar cells. Cells in the dorsal part of the PVCNd received more puncta than those in its ventral parts (Fig. 3, bar diagram). Additionally, labeled fascicles and fibers were observed in the PVCN and the intermediate acoustic stria. As in *Rhinolophus*, the PVCN of the mustached bat lacked immunopositive somata and the density of puncta was higher in the PVCNv than in the PVCNd (Fig. 3). In contrast to the horseshoe bat, however, no clearcut regional differences in puncta density within the PVCNd were noted.

DCN. The two subdivisions of the DCN of horseshoe bats, namely the dorsal non-laminated part (DCNd), where the CF-signal component is represented (Feng and Vater, '85), and the ventral laminated part (DCNv), where lower frequencies are represented, are clearly distinct in the immunostaining for GAD/GABA (Figs. 1, 2E,F, 3). The DCNd contains immunoreactive puncta but lacks immunopositive somata whereas the DCNv contains both labeled puncta and somata. Numerous immunoreactive cells are found in the fusiform and deep layers of the DCNv as shown in detail in Figure 2D,F. All immunopositive cells are distinctly smaller than the non-labeled fusiform projection neurons. In the outer fusiform cell layer, the majority of GAD/GABA-positive cells are intermediate in size (mean area $83 \mu\text{m}^2$, range $50\text{--}150 \mu\text{m}^2$) and are oval to round. Few small elongate somata were also labeled at the border to the molecular layer. In the deep layer of the DCNv immunostained round to oval cell bodies (mean area $75 \mu\text{m}^2$, range $50\text{--}166 \mu\text{m}^2$) were observed. In general, staining of proximal dendrites was weak so that the exact cell types could

not be further determined. Puncta density per unit area (Fig. 3, bar diagram) differed among the DCNv layers. The fusiform layer, particularly its outer region, had the highest density of labeled puncta. These puncta distinctly encircled or covered the somata of non-stained as well as immunopositive cells (Fig. 2D). The somata of non-stained large fusiform cells were also contacted by numerous puncta. The deep layer of the DCNv contained fewer puncta than the fusiform cell layer. Furthermore, these puncta were more diffusely distributed in the neuropil and on the somata of stained and non-stained cells. In the molecular layer, puncta were distributed in the neuropil and their density was less than in the fusiform layer. In the DCNd (Figs. 2E, 3), puncta density was moderate and the rather diffuse distribution of labeled puncta was similar to the pattern seen in the deep layer of DCNv.

The GAD/GABA-immunostain in the DCN of the mustached bat, which is laminated throughout its extent, qualitatively and quantitatively (Fig. 3) conforms to the pattern seen in the DCNv of the horseshoe bat.

Superior olive

The distribution of the GAD-stain in the nuclei of the superior olivary complex (SOC) is illustrated in Figure 4 (horseshoe bat) and Figure 5 (mustached bat). As a general feature, the periolivary nuclei are set apart from the principal nuclei by a higher density of stained puncta.

LSO. Numerous moderately immunostained cell bodies were observed within the main body of the LSO of the horseshoe bat (Fig. 4A). These cells were oval or round, ranging in size from 50 to $125 \mu\text{m}^2$ (mean area $99 \mu\text{m}^2$). There were slightly more immunostained cells in the lateral than in the medial limb of the LSO (Fig. 6). Typically, immunopositive as well as non-stained cells were contacted by relatively few puncta (mostly 3–4, up to 8) which were located on the somata and proximal dendrites (Fig. 4C). Some cells, however, did not receive any puncta. As compared to surrounding periolivary structures or other auditory centers, like CN or DNLL, labeling of punctate profiles in the LSO was relatively sparse and puncta distribution was more diffuse. Most of the immunostaining in the neuropil consisted of traversing fascicles or fibers. The LSO of *Pteronotus* (Figs. 5, 6) is similarly characterized by numerous moderately stained cells. These cells were most abundant in the dorsal and intermediate limb where puncta density was rather low. The dorsal margin of the ventral limb, however, received a remarkably high supply of immunostained puncta, almost matching that observed in periolivary areas (Fig. 5).

"Medial olivary nuclei." In *Rhinolophus*, the VMSO and DMSO are clearly distinct in their staining pattern for GAD (Figs. 4B, 6). The DMSO contained very few moderately GAD/GABA-immunoreactive cells, whereas the VMSO contained numerous such neurons (mean area $140 \mu\text{m}^2$, range $90\text{--}200 \mu\text{m}^2$). Their somata were spindle-shaped or multipolar (Fig. 4F) with oblique vertical orientation. Labeling of puncta was much more prominent in the DMSO than in the VMSO (Fig. 4D,F; Fig. 6, bar diagram). In *Pteronotus*, the MSO contained numerous moderately GAD/GABA-immunostained cell bodies throughout its extent (Figs. 5, 6) (mean area $130 \mu\text{m}^2$, range $106\text{--}180 \mu\text{m}^2$). These cells were either round or oval with the dendrites oriented perpendicular to the long axis of the nucleus. The soma shape and orientation of immunopositive cells thus closely resembled the projection cells in Nissl stain. Like the GAD/GABA-

Fig. 1. As shown on facing page. Schematic illustration of frontal sections through the brains of *Rhinolophus rouxi* (left) and *Pteronotus parnellii* (right) showing the main auditory centers and the respective distributions of GAD/GABA-immunoreactive (+) cells (filled circles; right side of the brain) and puncta (stippling; left side of the brain). The density of stippling indicates differential densities of puncta. Areas of very low puncta density (below 15 puncta/1,000 μm^2) are left empty. Calibration bar: 200 μm .

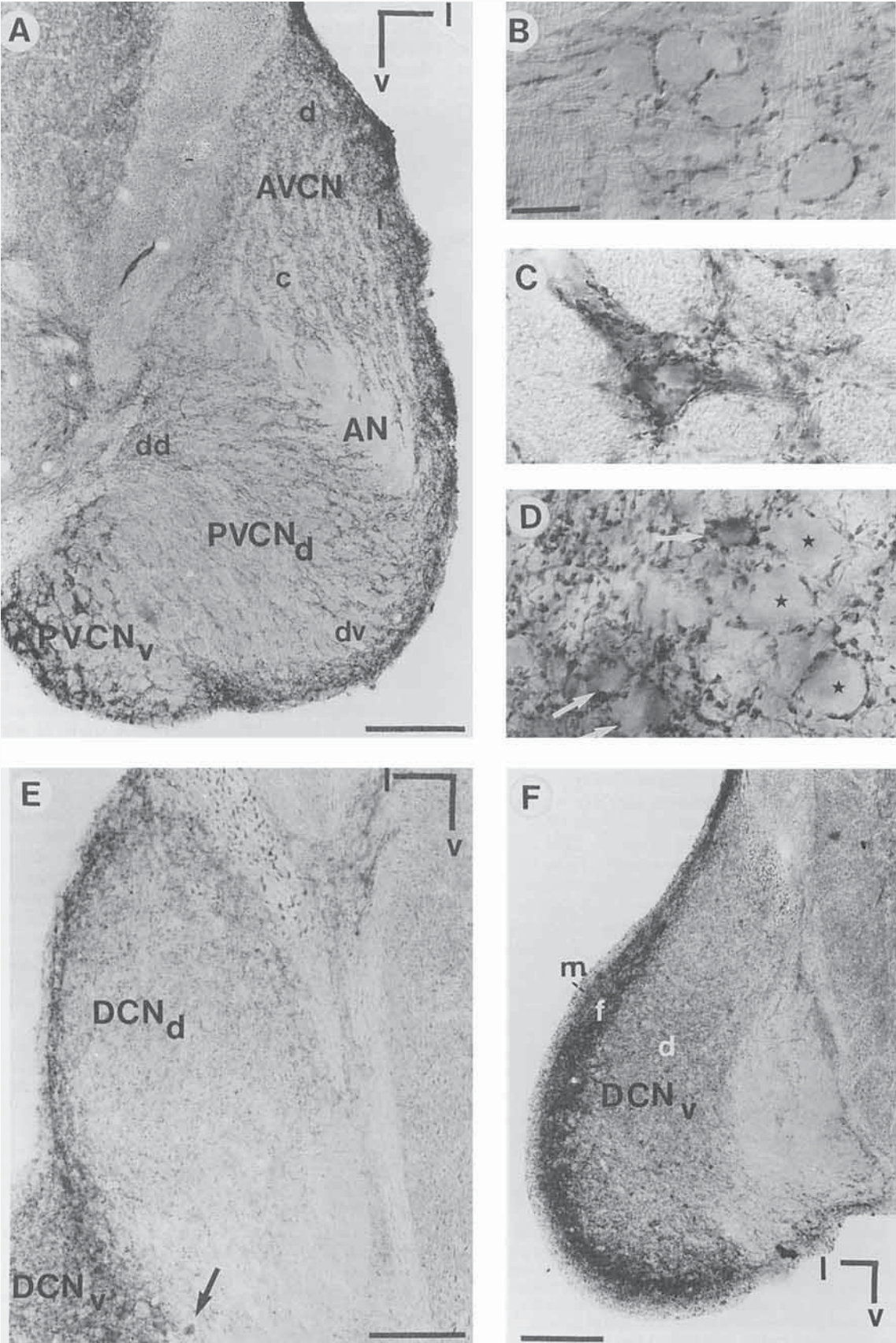


Figure 2

positive cells in the VMSO of *Rhinolophus*, these cells received few (2–4) or no puncta.

MNTB. A common feature of the MNTB of both species is the absence of labeled cell bodies (Fig. 6) and a relatively sparse supply of the somata of unlabeled principle cells with immunopositive puncta (2 to 8 puncta per cell) (Fig. 4E). Most of the label in the neuropil consisted of stained nerve fibers traversing in the trapezoid body.

Periolivary nuclei. The LNTB and VNTB contained numerous stained somata many of which were obscured by the high density of stained puncta (Figs. 4, 5). The periolivary nuclei giving rise to the olivocochlear bundle were also distinctly immunostained. In *Rhinolophus*, the N. olivocochlearis (NOC) is the sole origin of olivocochlear fibers which exclusively innervate the inner hair cells (e.g., Aschoff and Ostwald, '87). The NOC is distinctly outlined along the dorsal and medial margin of the LSO by a dense network of labeled puncta profiles (Fig. 4A) and contained numerous GAD/GABA-immunostained somata (Fig. 6). In *Pteronotus*, the lateral olivocochlear bundle arises from the interstitial nucleus (INT), which surrounds the dorsolateral margin of the LSO at caudal levels and the dorsal and dorsomedial margin of the LSO at more rostral levels (Bishop and Henson, '87). In these areas, puncta density was clearly higher than in the LSO and MSO (Fig. 5), however, compared to *Rhinolophus*, GAD/GABA-immunostained cells appeared less abundant (Fig. 6). Within the dorsomedial periolivary nucleus (DMPO), which gives rise to the medial olivocochlear bundle supplying the outer hair cells of the mustached bat (Bishop and Henson, '87), numerous GAD/GABA-immunostained somata were found and puncta density was high (Fig. 6).

Nuclei of the lateral lemniscus

In both species, the three subnuclei of the lateral lemniscus complex (DNLL, INLL, VNLL) distinctly differ in the GAD/GABA-label. Several details of the labeling pattern are species characteristic. This is shown by photomicrographs and schematic illustrations in Figures 7 and 8.

DNLL. The DNLL of both species (Fig. 7A,B) exhibits the most prominent staining pattern. Every cell in the DNLL appeared darkly immunostained with GAD/GABA-antibodies. This contrasts with all other auditory nuclei in

which GAD/GABA-positive cells only comprised a distinct subpopulation. In the horseshoe bat, immunostained cells in the DNLL formed a heterogeneous population as shown by the large range of somatic areas ($90\text{--}240\ \mu\text{m}^2$, mean $164\ \mu\text{m}^2$). In the lateral part of the DNLL of *Rhinolophus*, round to oval labeled cell bodies were densely packed (Fig. 7A,C) and covered by darkly stained puncta. In the medial part, which is composed of loosely packed cell columns within the ascending fibers of the lateral lemniscus, round and fusiform cells with horizontally oriented dendrites were labeled (Fig. 7A,D); these also received a dense supply of puncta. Most interestingly, the paralemniscal zone (PLZ) was also distinctly immunoreactive for GAD/GABA throughout its rostrocaudal extent. This zone is known to receive auditory input and functionally represents an auditory-vocal interface (Metzner, '89). The PLZ contained a mixture of oval and multipolar immunoreactive cells (range $60\text{--}270\ \mu\text{m}^2$, mean $118\ \mu\text{m}^2$) contacted by numerous puncta (Fig. 7A,E).

As shown in Figure 7B, the DNLL of *Pteronotus*, which forms a compact cell aggregate between the INLL and the IC is also prominently immunoreactive for GABAergic markers. Similar cell types as described for the DNLL in *Rhinolophus* were labeled. No separate PLZ is present in the mustached bat throughout most of the rostro-caudal extent of the lateral lemniscus complex. However, it was noted that the medial regions of the DNLL, particularly at its most rostral pole, contain immunopositive bipolar or multipolar cells, similar to those in the PLZ of *Rhinolophus* (Fig. 7H).

INLL. The INLL of *Rhinolophus* contained numerous GAD/GABA-positive cells which were more lightly stained than those in the DNLL (Fig. 7A,G). These cells (somatic area $75\text{--}231\ \mu\text{m}^2$, mean $116\ \mu\text{m}^2$) were organized into two clusters separated by a non-immunoreactive zone. Cells in the lateral cluster received fewer puncta than those in the medial cluster. The INLL of *Pteronotus* contained a prominent patch of dense puncta at its dorsolateral aspect and few moderately stained cells scattered throughout its extent (Figs. 7B, 8).

VNLL. The cytoarchitecture of the VNLL of *Pteronotus* and *Rhinolophus* shows species specific differences (Schweizer, '81; Vater and Feng, '90; Zook and Casseday, '82a). GAD/GABA-immunocytochemistry also revealed subregional specializations. In *Rhinolophus*, the lateral subdivision of the VNLL (l) contained many stained cell bodies of oval to fusiform shape (somatic area $62\text{--}132\ \mu\text{m}^2$, mean $101\ \mu\text{m}^2$), which were contacted by numerous puncta. Immunostaining was most prominent in a dorsal band along the border with the INLL (Fig. 7A,F). In contrast, the medial subdivision of the VNLL (m) (Figs. 7A, 8), which is known to receive calyciform synapses from PVCN-axons (Vater and Feng, '90), did not contain immunopositive cell bodies. Immunostained puncta were less numerous than in the lateral VNLL, although density of cell packing in Nissl stain is higher. In *Pteronotus*, the dorsal subdivision of the VNLL (d) contained many moderately labeled somata and dense puncta. In the ventral subdivision (v), puncta density was much lower and only a few stained somata were arranged in bands (Figs. 7B, 8). The ventral subdivision is known to receive large calyciform endings (Zook and Casseday, '85), and in this feature corresponds to the medial subdivision of the VNLL in the horseshoe bat.

Fig. 2. Photomicrographs of the GAD-immunostain in the cochlear nucleus of *Rhinolophus* (frontal sections). **A:** Anteroventral (AVCN) and posteroventral (PVCN) cochlear nucleus. Note the different densities of labeled puncta within cytoarchitectonic subregions: dorsal (d), lateral (l), and central (c) AVCN; dorsal (dd) and ventral (dv) subdivision of PVCN as compared to PVCNv. Calibration bar: 200 μm . **B:** GAD-immunostained puncta form perisomatic rings around non-labeled spherical cells in the central AVCN. **C:** GAD-immunostained puncta cover the somata of a non-labeled multipolar cell of the PVCNv and distinctly outline the proximal dendrites. **D:** GAD-immunostained somata (arrows) and puncta in the fusiform cell layer of the DCNv. Puncta encircle the somata of non-labeled fusiform projection cells (asterisks). In outer regions of the fusiform cell layer (towards left) numerous puncta are observed in the neuropil and on somata of immunostained cells. B–D, calibration bars = 10 μm . **E:** Specialized dorsal non-laminated portion of the DCN (DCNd). There are no immunostained cell bodies, except at the border to DCNv (arrow). Calibration bar = 100 μm . **F:** Ventral laminated portion of the DCN (DCNv). Note the high density of puncta in the outer fusiform cell layer (f), which masks immunostained cell bodies. In the deep layer (d), few immunoreactive cells are present. m: molecular layer. Calibration bar = 200 μm .

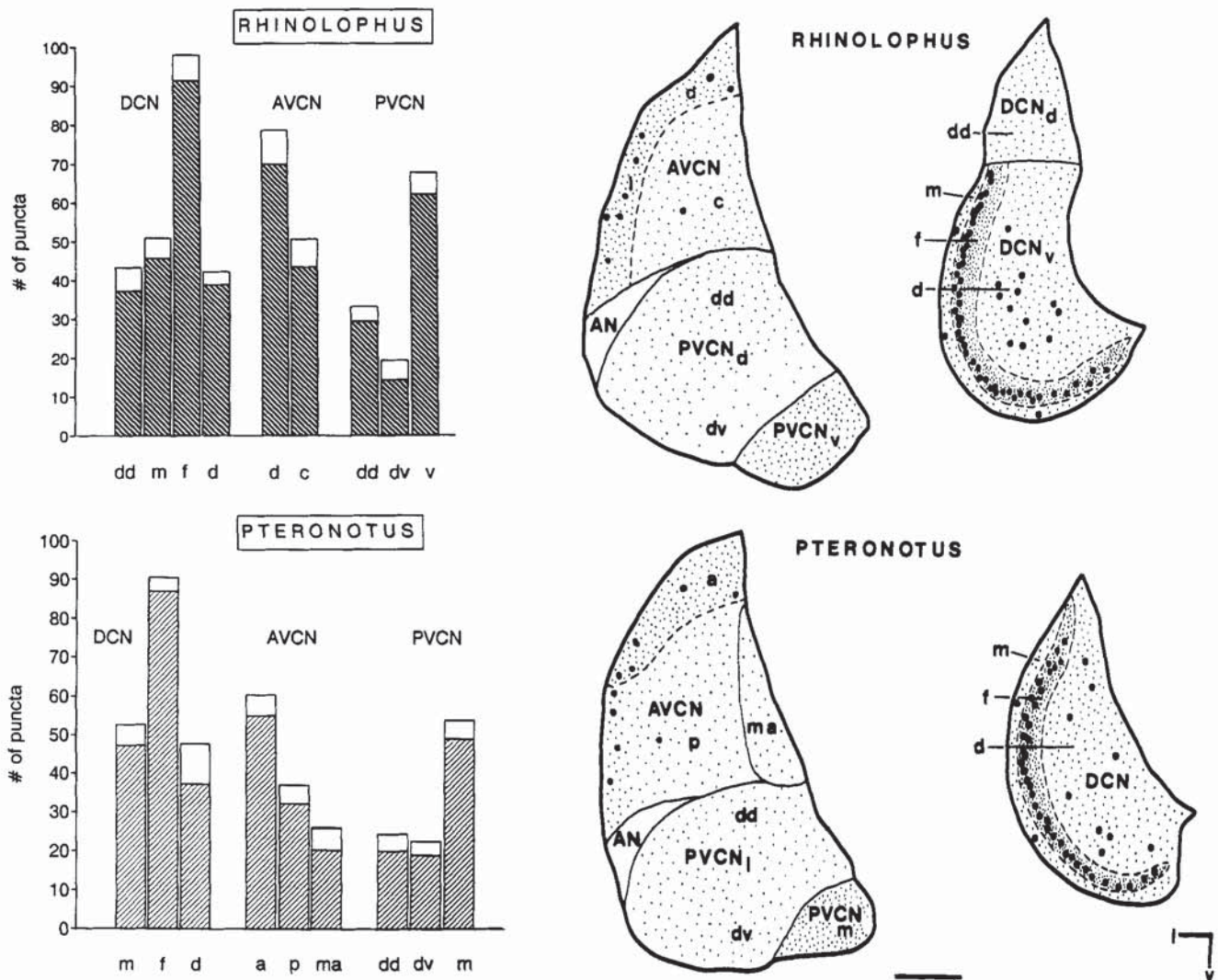


Fig. 3. **Left:** The bar diagrams compare the densities of GAD/GABA-immunostained puncta per 1,000 μm^2 in the subdivisions of the cochlear nucleus of *Rhinolophus* (top) and *Pteronotus* (bottom). Positive standard deviations are indicated by white areas. DCN: m, f, d refer to the molecular, fusiform and deep layers of the DCNv of *Rhinolophus* and the DCN of *Pteronotus*; dd refers to the DCNd of *Rhinolophus*;

AVCN: d, c refer to the dorsal and central division (*Rhinolophus*); a, p refer to the anterior and posterior division (*Pteronotus*); PVCN: dd and dv refer to the dorsal and ventral regions of the PVCN; v refers to the PVCNv. **Right:** Schematic drawings of frontal sections show the distributions of labeled cells (circles) and regions of high puncta densities (stippling) for both species. Calibration bar = 200 μm .

Inferior colliculus

The inferior colliculus (IC) of both bats was characterized by a large heterogeneous population of darkly stained GAD/GABA-positive cells (Figs. 1, 9–13). Immunostained cells were located in the central nucleus (ICc) and in the external nucleus (ICx). GAD/GABA-positive puncta were observed in the neuropil as well as on GAD/GABA-positive cells and non-stained cells. In the ICc of both bats, subregional differences in immunostaining were seen. In the horseshoe bat (Figs. 9, 11), there was a distinct band of sparse puncta extending dorsoventrally along the lateral part of the ICc, which was continuous with a distinct region of low puncta labeling in ventral aspects of the rostral ICc. In contrast, puncta density in the dorsal (d) and ventromedial (vm) parts of the ICc was rather high. In order to assess whether these regional differences correspond to differences in cell

density in different areas, cell density per 1000 μm^2 was counted in Nissl stained paraffin material. Cell density in the ventral ICc was less than in other regions by a factor of two, whereas the difference in GAD/GABA-positive puncta supply amounted to a factor of 8. Figure 10 illustrates the regional differences in immunopositive cell types and their respective puncta supply. The dorsal ICc (Fig. 10B) contained a heterogeneous population of round to fusiform and multipolar cells mostly of intermediate size, which received numerous puncta (see also Figs. 9C, 11). The ventromedial ICc (Fig. 10D) likewise contained a mixture of different cell types, but the number of large fusiform types is increased (see also Fig. 11). All cells were contacted by numerous puncta either on the somata or preferentially on the proximal dendrites. The ventral regions (Fig. 10C) contained mostly intermediate-sized fusiform and multipolar

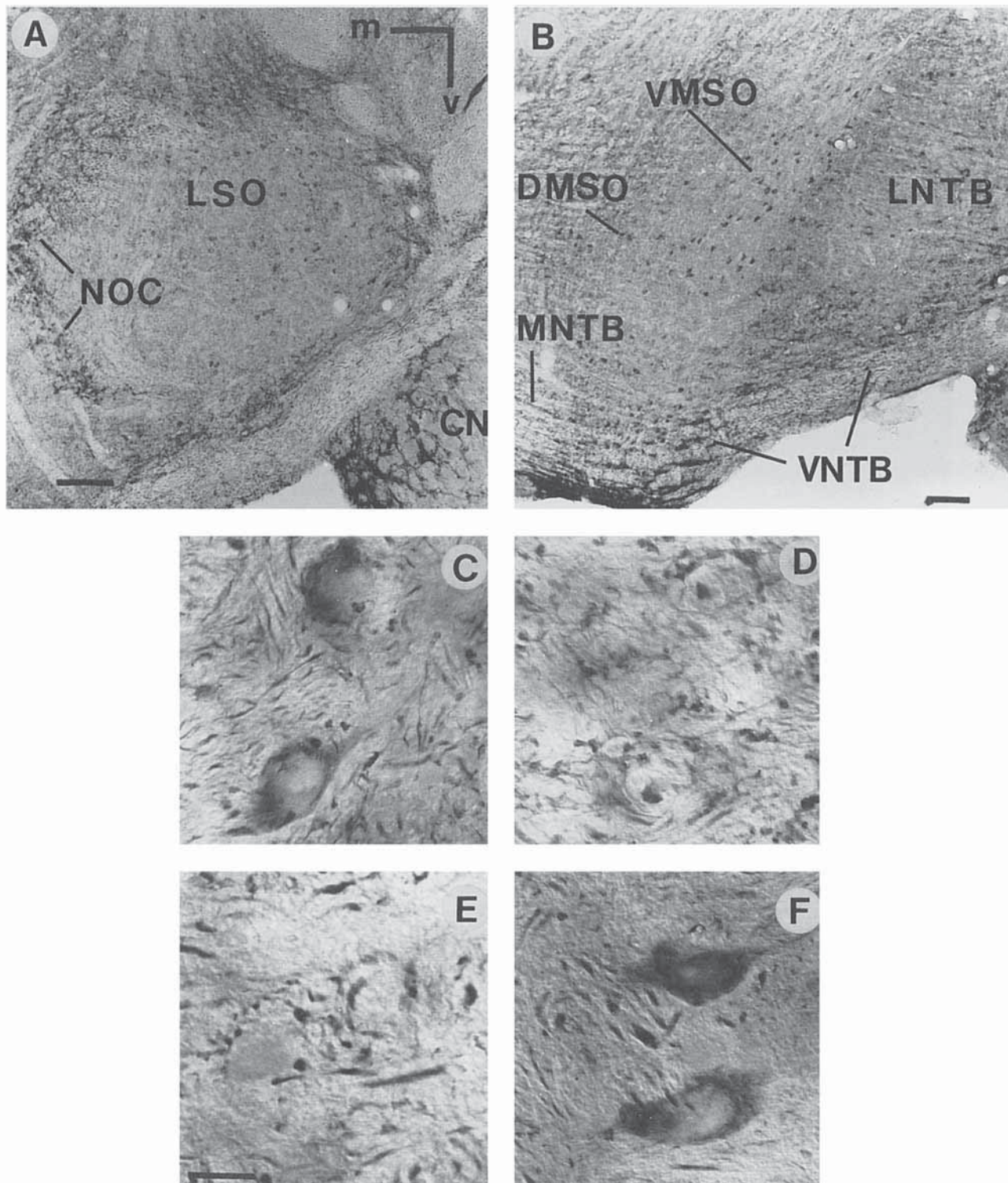


Fig. 4. Photomicrographs of the GAD-immunostain in the superior olivary complex (SOC) of *Rhinolophus* (frontal sections). **A:** Low power picture of the LSO whose medial margin is surrounded by the NOC. **B:** Low power picture of a more rostral section showing the VMSO and DMSO, the MNTB and periolivary regions of VNTB and LNTB. Note that all periolivary regions are characterized by a high puncta density which masks labeled somata. **C–F:** High power photomicrographs of the immunostain in the main nuclei of the SOC. **C:** GAD-immunoreac-

tive cells and puncta in the LSO. Labeled puncta are present in the neuropil and close to the somata of LSO-cells. **D:** GAD-immunoreactive puncta in the DMSO form clusters in the neuropil. **E:** GAD-immunoreactive puncta encircle a non-stained neuron in the MNTB. **F:** GAD-immunoreactive bipolar cells in the VMSO. In the neuropil, numerous profiles of labeled fibers but only very few puncta are observed. Calibration bars: A, B = 100 μ m; C–F = 10 μ m.

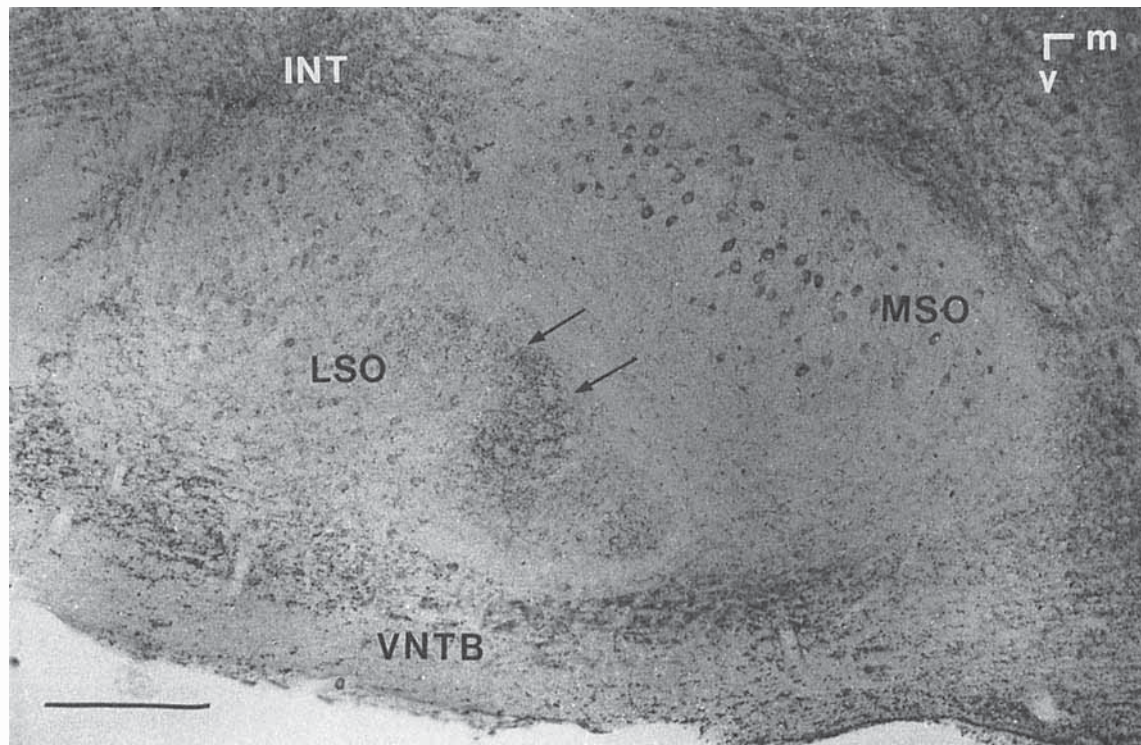


Fig. 5. Photomicrograph of the GAD-immunostain in the superior olivary complex (SOC) of *Pteronotus* (frontal section). Puncta staining is more prominent in periolivary structures than in the main nuclei of the SOC. However, within the dorsal margin of the ventral limb of the

LSO (arrows), puncta staining almost matches that observed in the periolives. Moderately immunostained cells are present in LSO and MSO and within periolivary structures. Calibration bar = 200 μm .

immunoreactive cells, that were either free of or had very few labeled puncta (see also Figs. 9B, 11). These differences suggest different functional properties. It was further noted that the dendritic processes of bipolar cells were commonly oriented within the fibrodendritic lamina while those of multipolar cells crossed the laminae.

The immunostaining pattern in *Pteronotus* is shown in Figures 12 and 13. Throughout the ICc, a heterogeneous population of immunostained cells was found which comprised large bipolar, multipolar, and smaller round to oval cells. Similar to *Rhinolophus*, ventral parts of the ICc contained mostly intermediate sized cells which received a relatively low puncta supply. These regions partially correspond to the anterolateral division (al), but in most caudal sections seem to encompass parts of the dorsoposterior (dp) and medial (m) division (Fig. 12). As in the ICc of *Rhinolophus* there were clear regional variations in the density of puncta within the ICc. A band of low puncta density forms a vertical stripe on the lateral aspect of the dorsoposterior division (Fig. 12) and along the anteriorlateral division in more rostral sections.

Medial geniculate body

There were pronounced differences in the GAD/GABA-staining of the MGB in horseshoe bats and mustached bats (Figs. 1, 14, 15). In *Rhinolophus*, all subdivisions of the MGB (d, v, m) contained numerous GAD/GABA-positive somata. In *Pteronotus* only few labeled somata were ob-

served which were confined to the dorsal subdivision and scattered along the lateral margin of the MGB (Figs. 14B, 15). In *Rhinolophus*, GAD/GABA-positive cells in the three subdivisions of the MGB comprised a heterogeneous population. Soma shape was round to oval and somatic areas were mostly smaller than those of non-labeled cells, ranging from 25 to 150 μm^2 . Mean somatic sizes were not significantly different among subdivisions, but immunopositive cells were most numerous in the ventral subdivision (Fig. 15). The immunostained cells had excentric nuclei and sparse perikaryal cytoplasm and were often characterized by a pronounced staining of one or two dendrites (Fig. 14A,C). Occasionally complex dendritic appendages were observed in neurons of the dorsal as well as ventral division. In the ventral division, these dendritic appendages were in close apposition to the somata of neighboring cells (Fig. 14C). The immunopositive cells received a varying amount of puncta (0 up to ten). Morphology of labeled cells in the dorsal division of the MGB of *Pteronotus* closely resembled the immunopositive cells in the dorsal MGB of *Rhinolophus* (Fig. 14A,B), although their somata were slightly larger.

Immunostained puncta were observed throughout the MGB, in both species and regional differences in puncta density and pattern were noted. In *Rhinolophus*, the neuropil of the dorsal and ventral division contained numerous immunopositive dendritic profiles, which were often contacted by of puncta. Further immunostained puncta were located on the somata of non-labeled cells and in the

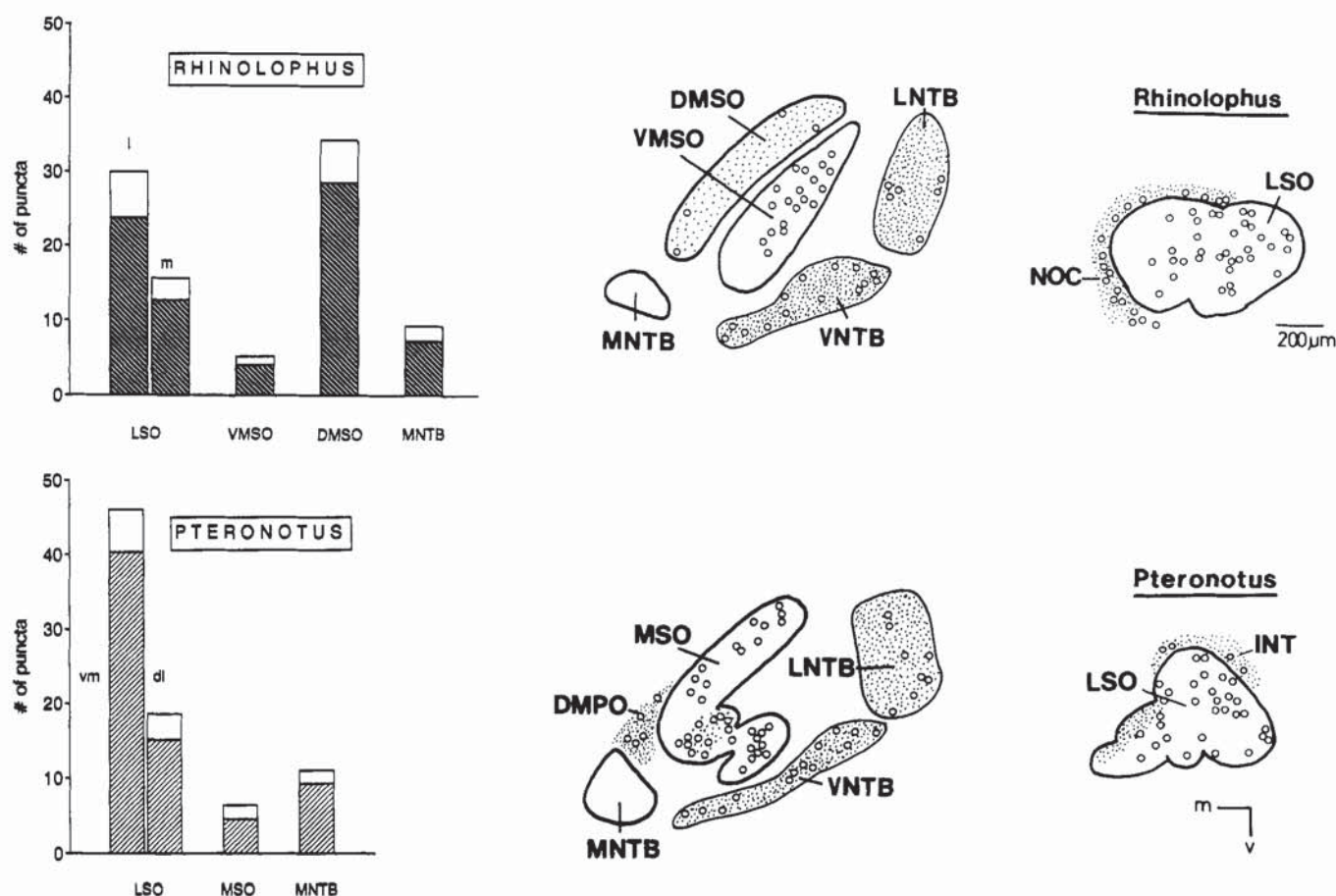


Fig. 6. **Left:** The bar diagrams compare the densities of GAD-immunostained puncta per $1,000 \mu\text{m}^2$ in the main nuclei of the superior olivary complex (SOC) of *Rhinolophus* (top) and *Pteronotus* (bottom). Positive standard deviations are indicated by white areas. **Right:**

Schematic illustrations of the GAD/GABA-immunostain in the SOC at the level of the LSO and in a more rostral section, respectively for both species. Immunostained cell bodies are indicated by circles, regions of high densities of immunostained puncta are indicated by stippling.

neuropil (Fig. 14A,C). The medial subdivision was characterized by an abundance of coarse puncta encircling the somata of non-stained cells (Fig. 14E). Gross analysis of puncta densities showed that the dorsal subdivision contained slightly fewer puncta than the medial and ventral subdivisions. The latter did not differ significantly in their puncta content (Fig. 15, bar diagrams). In dorsal and ventral subdivisions, regional variations in puncta densities were observed, a feature which deserves further analysis. In *Pteronotus*, gross analysis of puncta densities in the dorsal and ventral subdivisions did not reveal prominent differences (Fig. 15, bar diagrams), but it was noted that ventral aspects of the dorsal subdivision (Fig. 14B) contained clearly fewer puncta than dorsal and lateral regions or other subdivisions (Fig. 14D,F). Puncta density in the medial subdivision was slightly higher than in other regions (Fig. 15, bar diagrams). The pattern of puncta labeling showed clear regional differences (Fig. 14B,D,F). Ventral parts of the dorsal subdivision were characterized by a scattered arrangement of mostly fine puncta profiles (Fig. 14B). In the ventral subdivision, an intricate network of labeled axons characterized by numerous varicosities was present (Fig. 14D). The medial subdivision contained coarser puncta than the other subdivisions (Fig. 14F).

DISCUSSION

General features

The basic pattern of immunostaining in the nuclei of the ascending auditory pathway of the two CF-FM bats is in agreement with data from other mammalian species. The comparative analysis reveals the following salient features:

1. Putatively GABAergic neuronal elements are found throughout the auditory pathway, but the prominence of label among the various auditory centers differs quantitatively as well as qualitatively. These differences are expressed by the presence or absence of populations of labeled cells, and the supply of immunostained puncta.

2. Many auditory centers are characterized by subregional differences in immunostaining which correlate with species characteristic details of cytoarchitectonical organization, connectivity and/or tonotopic representation patterns.

3. Prominent species-specific specializations in the organization of putatively inhibitory networks are noted at the level of the DCN in the horseshoe bat and the MGB in the mustached bat. These features will be addressed in detailed discussions of the individual auditory centers.

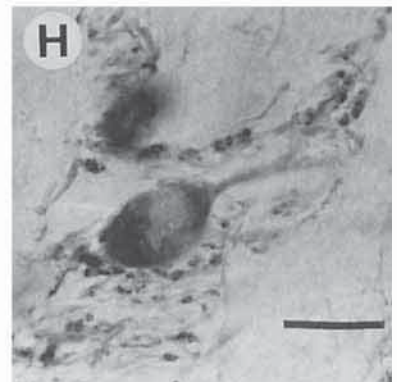
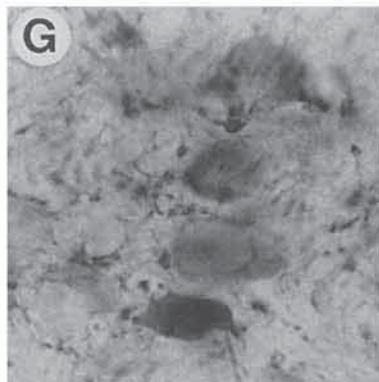
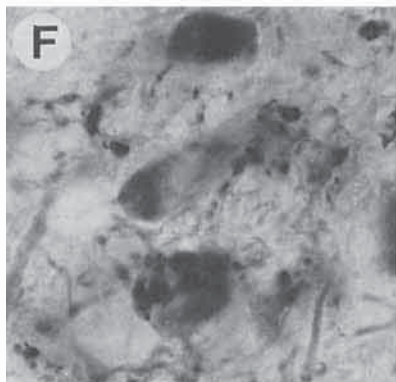
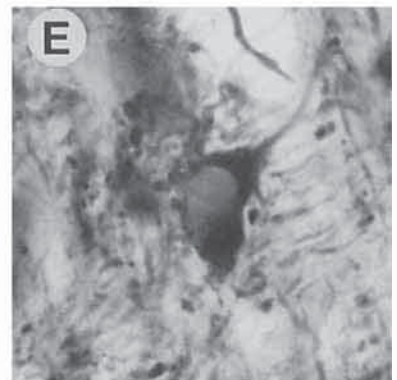
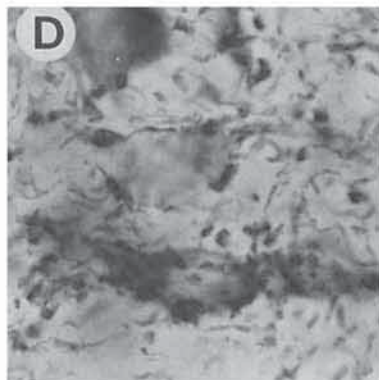
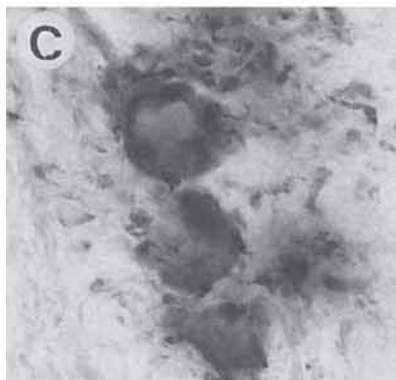
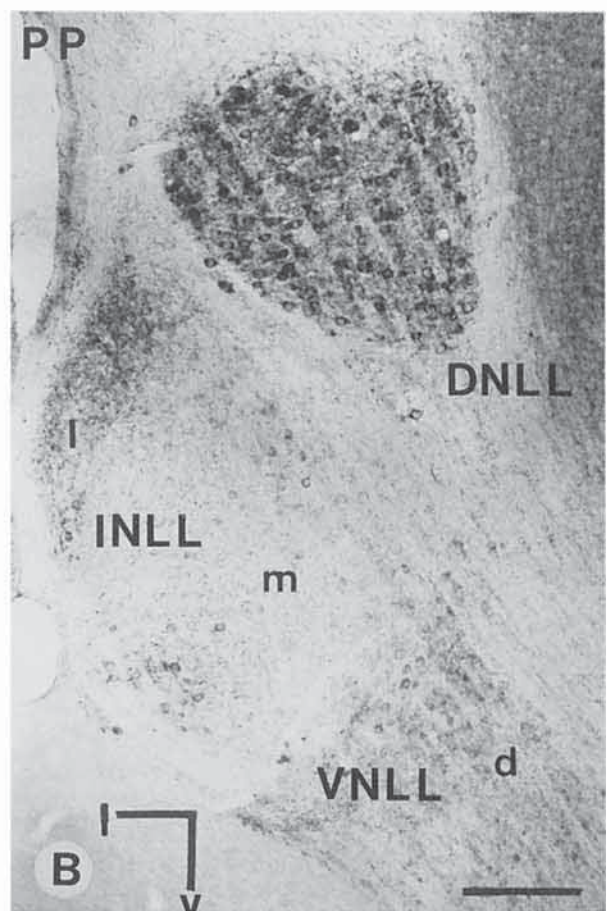
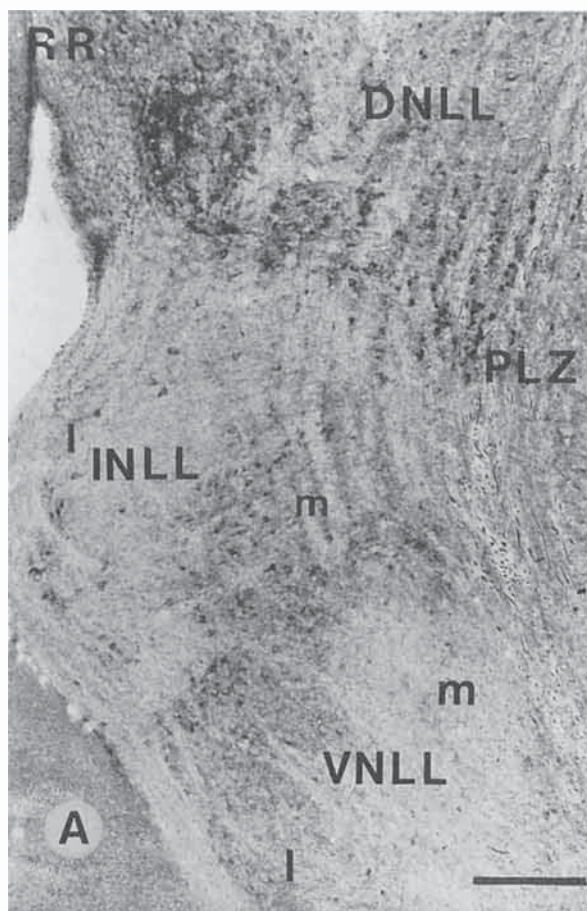


Figure 7

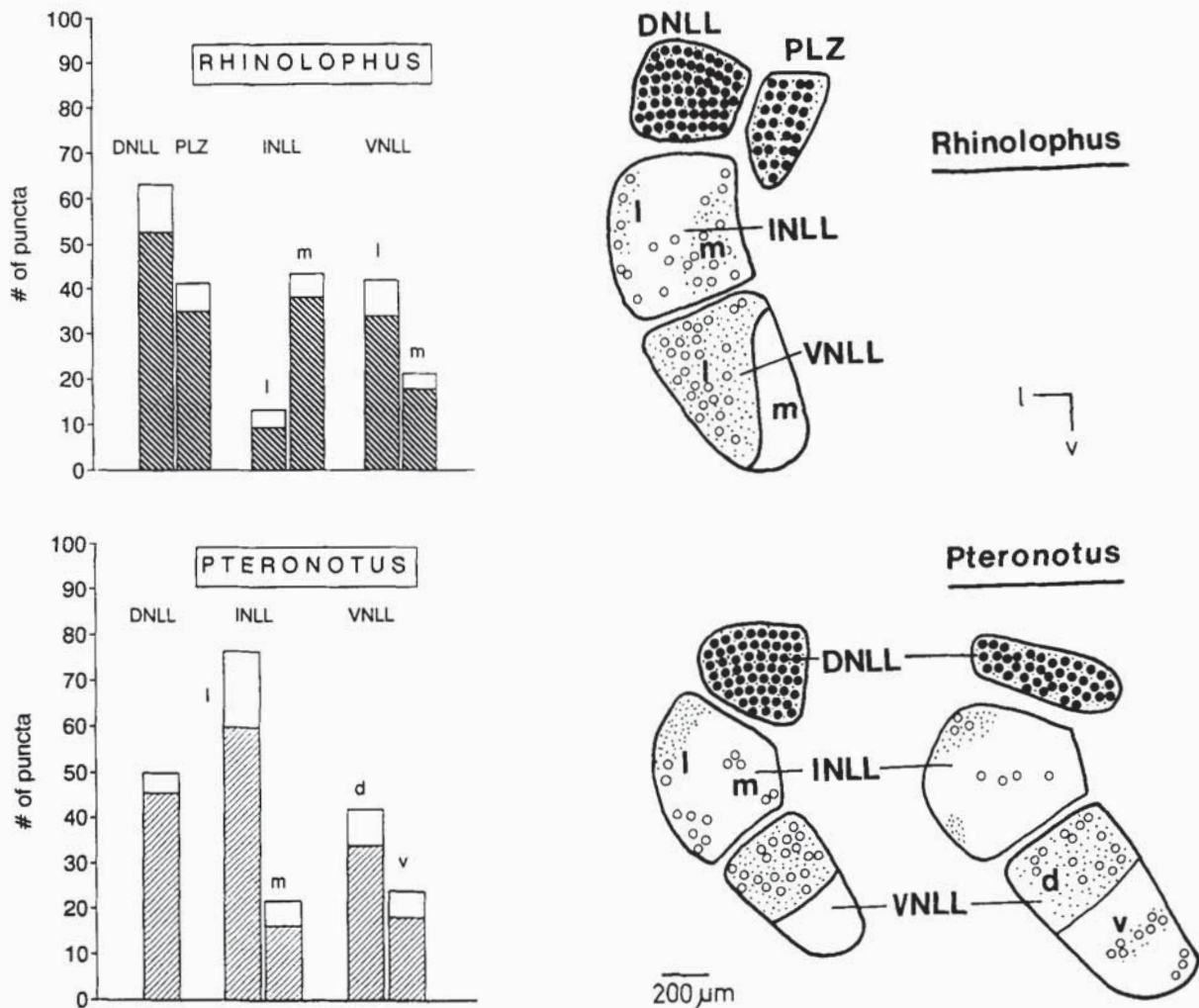


Fig. 8. **Left:** The bar diagrams compare the densities of GAD-immunostained puncta per $1,000 \mu\text{m}^2$ in the subnuclei of the lateral lemniscus (LL) of *Rhinolophus* (**top**) and *Pteronotus* (**bottom**). Positive standard deviations are indicated by white areas. **Right:** Schematic drawings of frontal sections through the LL of both species showing the

distributions of immunostained cells (filled circles: darkly stained somata; open circles: moderately stained cells) and regions of high puncta densities (stippling). For *Pteronotus*, two sections at different rostro-caudal locations are shown (**left section:** caudal).

Fig. 7. Photomicrographs of the GAD-immunostain in the nuclei of the lateral lemniscus (LL). **A,B:** Low power photomicrograph of the LL of *Rhinolophus* (RR) and *Pteronotus* (PP); l, m refer to lateral and medial regions of the INLL (both species) or VNLL (*Rhinolophus*); d refers to the dorsal division of the VNLL in *Pteronotus*. **C-E:** High power photomicrographs of the immunostain in the subdivisions of the LL. **C:** GAD-positive cells surrounded by immunopositive puncta in the lateral DNLL of *Rhinolophus*. **D:** GAD-positive round and bipolar cells in the medial DNLL of *Rhinolophus*. Numerous puncta are located in the neuropil and along the somata and dendrites of immunopositive cells. **E:** In the PLZ of *Rhinolophus*, GAD-positive puncta are located in the neuropil and along the somata of immunopositive cells. **F:** GAD-positive cells in the lateral VNLL of *Rhinolophus*. Clusters of coarse puncta are observed on cell somata and in the neuropil. **G:** GAD-positive cells in the INLL of *Rhinolophus*. Coarse and fine puncta are found in the neuropil and close to cell bodies. **H:** GAD-positive cells in the medial part of the DNLL of *Pteronotus*, which appear similar to the immunopositive cells in the PLZ (**E**) of *Rhinolophus*. Puncta are located close to cell bodies and form fine strands in the neuropil. Calibration bars: A,B = $200 \mu\text{m}$; C-H = $10 \mu\text{m}$.

Cochlear nucleus

In several mammalian species, the subdivisions of the CN have been shown to possess characteristic distributions of GAD/GABA-immunoreactive somata and puncta (rat: Mugnaini, '85; guinea pig: Peyret et al., '86; Wenthold et al., '86; gerbil: Roberts and Ribak, '87; cat: Adams and Mugnaini, '87; Saint Marie et al., '89a).

Distributions of immunostained cells. Our data agree with previous findings that putatively GABAergic neurons are less abundant in the AVCN and PVCN than in the DCN (e.g., Wenthold et al., '86). Consistent with this, inhibitory interactions are less pronounced in the ventral CN than in the DCN (review: Caspary, '86). It is unknown whether the few immunopositive cells in the AVCN are projection neurons or involved in local inhibitory interaction. In the DCN, all studies demonstrated the presence of putatively GABAergic cells in the superficial layer (cartwheel and

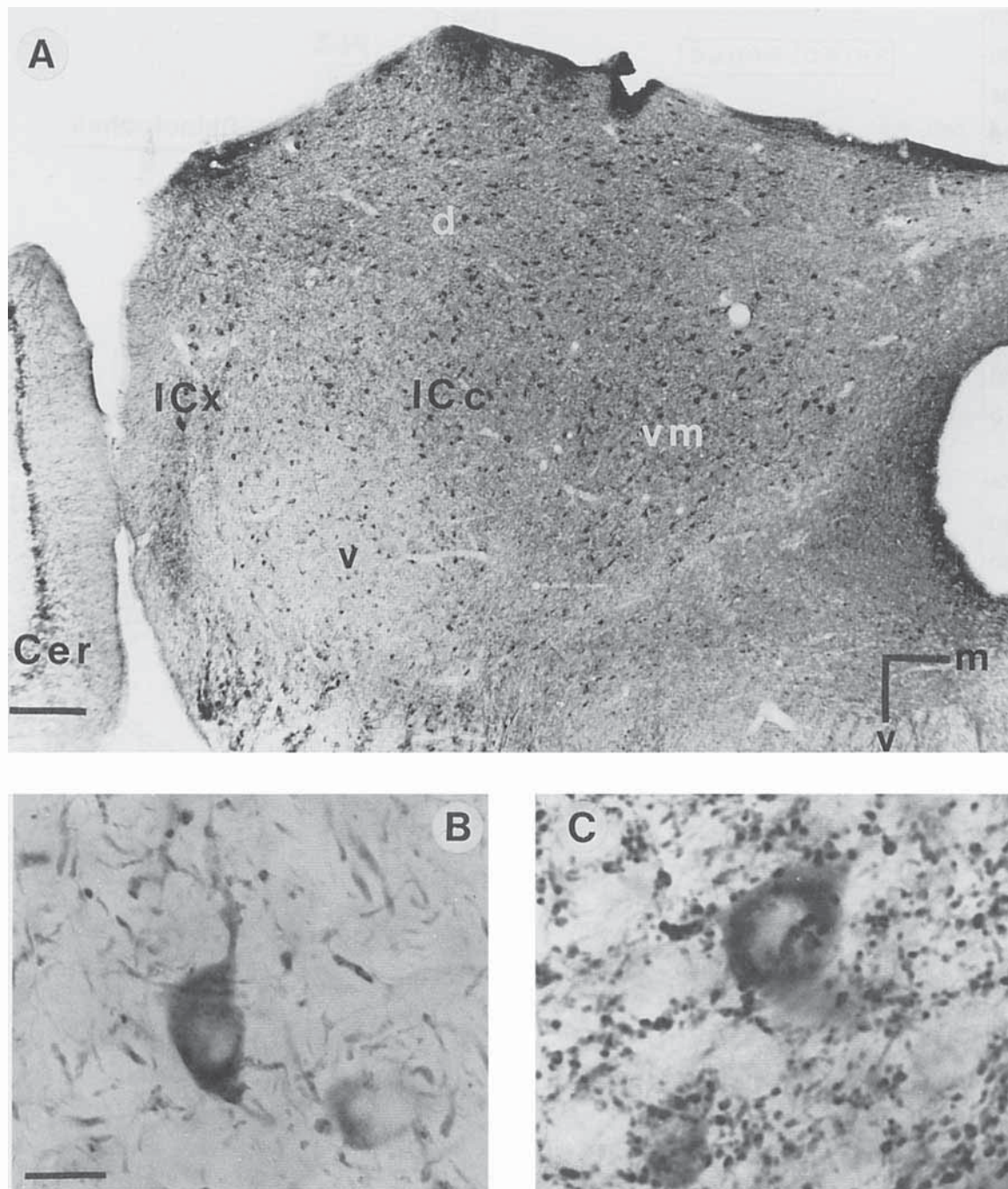


Fig. 9. Photomicrographs of the GAD-immunostain in the inferior colliculus (IC) of *Rhinolophus*. **A:** Low power photomicrograph of the IC. Immunostained somata are present throughout the central nucleus (ICc) and the external nucleus (ICx). Puncta staining is strong in the ICc, but not homogenous: areas of low puncta densities are located in the ventral ICc (v) and along the lateral margin of the ICc; d, v, vm refer to dorsal, ventral and ventromedial subregions of the ICc; Cer: cerebellum. Calibration bar = 200 μ m. **B:** High power photomicrograph of GAD-immunopositive cells in the ventral ICc. Few puncta are observed in the neuropil and on cell dendrites. **C:** High power photomicrograph of GAD-immunopositive cells in the dorsal ICc. Somata of immunopositive and non-stained cells are covered by numerous puncta. Calibration bars: B, C = 10 μ m.

stellate cells) and the deep layer (Golgi cells and few giant cells) (Mugnaini, '85; Peyret et al., '86; Wenthold et al., '86; Roberts and Ribak, '87; Adams and Mugnaini, '87). Cartwheel and stellate cells are involved in local inhibitory

circuits influencing the fusiform projection neurons (Osen and Mugnaini, '81). Their dendrites receive input from granular cell axons which are orderly organized in the molecular layer. The distribution of cells in the DCNv of

Rhinolophus

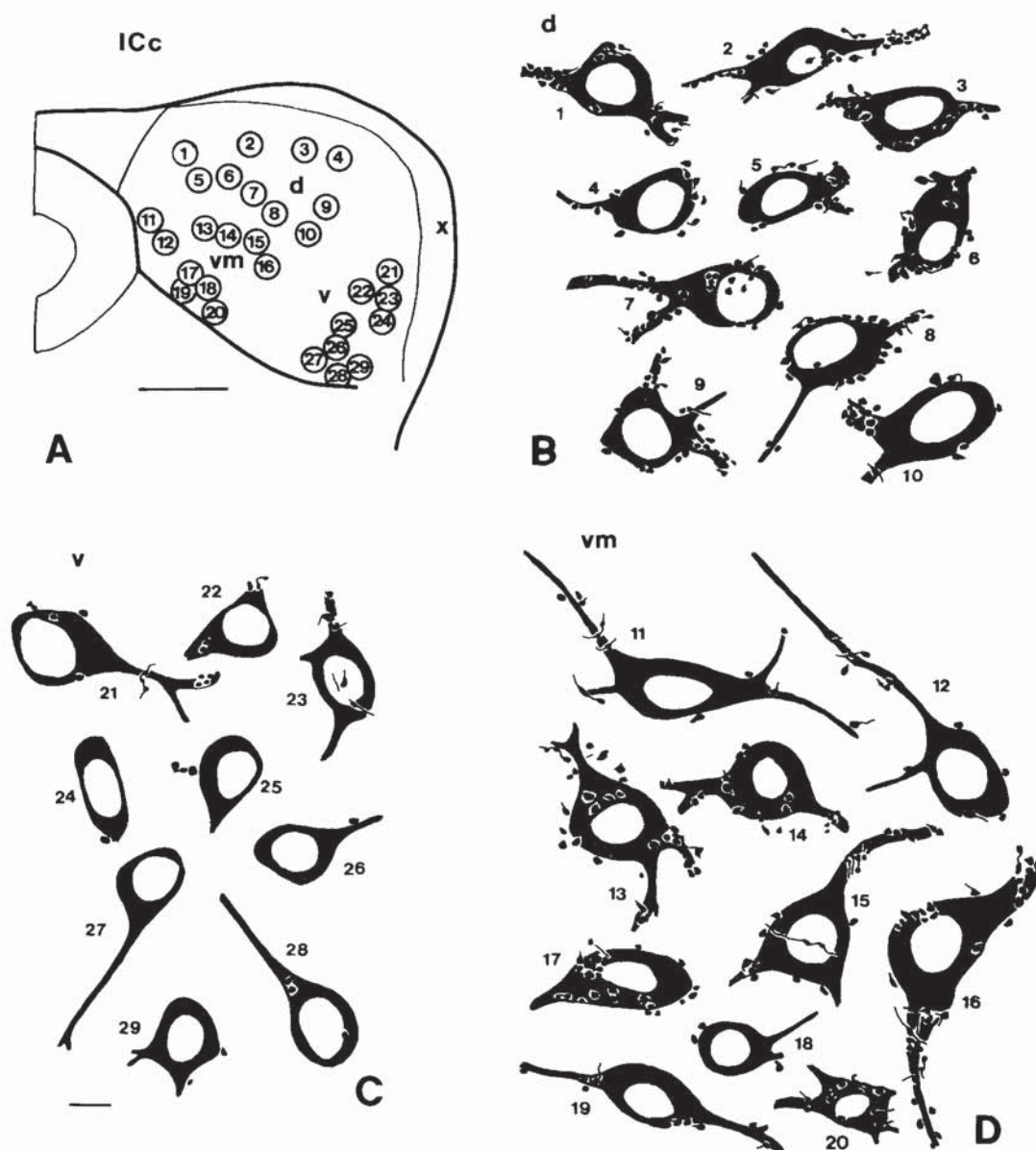


Fig. 10. Drawings of GAD-immunostained cell bodies and their puncta supply in different regions of the ICc of *Rhinolophus*. A: Survey drawing of the location of the cells shown in B–D. The numbers refer to the location of the respective cells within the ICc. B: Cell types in the

dorsal region of the ICc (d). C: Cell types in the ventral region of the ICc (v). D: Cell types in the ventromedial region of the ICc (vm). Calibration bars: A = 200 μ m; B–D = 10 μ m.

horseshoe bats and the DCN of mustached bats is similar to that observed in other mammals. Although we were unable to clearly identify the labeled cell types, this suggests the presence of similarly structured inhibitory circuits. Given the wiring scheme proposed above, the lack of GAD/GABA-immunoreactive cells in the specialized DCNd of the horseshoe bat appears linked to the absence of lamination. Species-specific differences in the lamination of the DCN (e.g., the poor lamination of the DCN in primates or whales

as compared to the prominent lamination of the DCN in cats or rodents), appear correlated with different degrees of development of the granular cell system (Osen and Mugnaini, '81). Consequently, the lack of a distinctly organized granular cell system in the DCNd of the horseshoe bat not only creates an ill-ordered morphological appearance but is also accompanied by a disappearance of transmitter-specific local inhibitory circuits. It is possible that a similar situation exists in the non-laminated DCN of primates. As

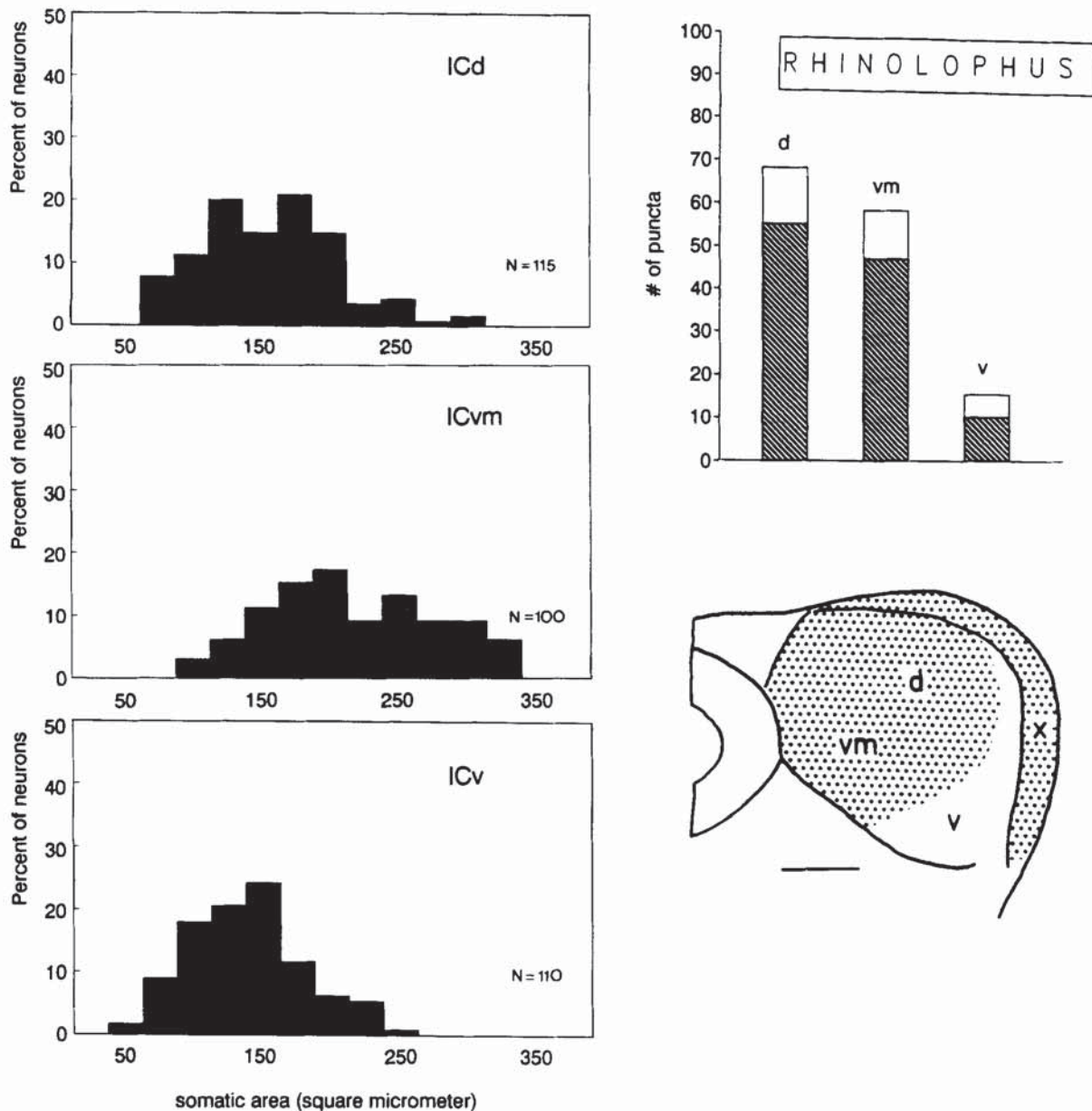


Fig. 11. Comparison of the size of GAD-immunoreactive cells (black bars) and puncta densities (obliquely shaded bars) in different subregions of the ICc of *Rhinolophus*. The inset schematically shows the regions of high puncta densities (shaded areas). Same abbreviations as in Figure 9.

discussed in Vater et al. ('92), the horseshoe bat DCN could serve as a model for comparison of information processing within a laminated and a non-laminated DCN.

Puncta distributions. All subdivisions of the CN receive a dense supply with GAD/GABA-immunoreactive terminals. In bats, as in other mammals, there are regional differences in puncta density which correlate with cell packing density as well as with the distribution of particular cell types (e.g., Wenthold et al., '86; Saint Marie et al., '89a). Characteristic differences in puncta morphology on different cell types or subdivisions have suggested that puncta originate from more than one pathway. One possible source is the population of GAD/GABA-immunopositive cells intrinsic to the CN. In the DCN of *Pteronotus* and

the DCNv of *Rhinolophus*, axonal boutons of GAD/GABA-immunoreactive local interneurons are expected to contribute to inhibitory circuits. For the ventral CN, the intranuclear frequency specific pathway arising in the deep layer of DCN (Feng and Vater, '85; Wickesberg and Oertel, '88) could represent a possible candidate. However in the guinea pig, this pathway is formed primarily by glycinergic neurons of the deep DCN (Saint Marie et al., '91). In *Rhinolophus*, a similar situation seems to exist: the DCNd as well as the deep layer of the DCNv contain a large population of glycine-immunoreactive cells (Vater et al., '92) whose morphology resembles the cells giving rise to the intranuclear pathway to the ventral CN (Feng and Vater, '85). Other sources of GABAergic input are the periolivary cell groups

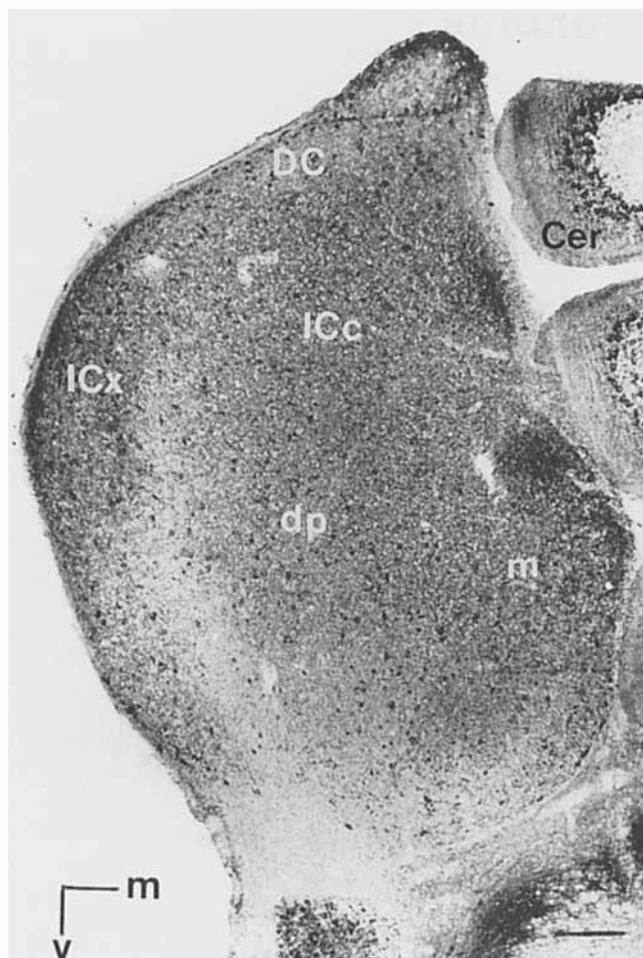


Fig. 12. Low power photomicrograph of the GAD-immunostain in caudal aspects of the inferior colliculus (IC) of *Pteronotus*. Immunopositive cells are found throughout the dorsoposterior (dp) and medial (m) division of the central nucleus (ICc), in the external nucleus (ICx), and the dorsal cortex (DC). Staining of puncta is strong in the external nucleus and throughout most of the central nucleus. A vertical oriented band of low puncta density is located along lateral parts of the dp. Further regions of low puncta density are found in ventral parts of the central nucleus. Cer: cerebellum. Calibration bar = 200 μ m.

projecting to the CN (Vater and Feng, '90; Spangler et al., '87; Winter et al., '89). In bats as well as in other mammals (e.g. Helfert et al., '89), the LNTB and VNTB contain numerous GABAergic cells. As discussed for other species (Caspary, '86; Adams and Mugnaini, '87; Saint Marie et al., '89a), periolivary neurons are putative candidates for origin of the extrinsic GABAergic input to the CN.

Superior olivary complex

The LSO and the MNTB are integral parts of the pathway analysing interaural intensity differences (review: Irvine, '86) and their functional organization in bats conforms well with the typical mammalian pattern (Casseday et al., '88; Covey et al., '91). The LSO of all investigated mammals contains a subpopulation of putatively GABAergic cells. In most species, including the bats studied here, these cells closely resemble projection cells providing input to the IC (guinea pig: Thompson et al., '85; Helfert et al.,

'89; gerbil: Roberts and Ribak, '87; cat: Saint-Marie et al., '89b). In the cat, a projection of putatively GABAergic LSO-cells to the IC has been demonstrated directly by combined HRP-tracing and GABA-immunochemistry (Saint-Marie et al., '89b). Species differences do, however, exist in the relative proportion of GAD/GABA-immunoreactive cells in LSO; this suggests differences in the contribution of LSO-neurons to GABA-mediated inhibition in the IC (Helfert et al., '89). In the rat, the morphology of GABA-immunoreactive LSO-cells clearly differs from the principal projection neurons and their distribution suggests a participation in the lateral olivocochlear system (Moore and Moore, '87). The MNTB of all species studied does not contain cells immunoreactive for GABA-markers (Thompson et al., '85; Peyret et al., '86; Moore and Moore, '87; Roberts and Ribak, '87; Adams and Mugnaini, '90), instead all of its cells are immunoreactive for glycine (e.g., Wenthold et al., '87; Helfert et al., '89; Adams and Mugnaini, '90; Vater et al., '90) providing contralateral inhibitory input to LSO-neurons. Both LSO and MNTB are characterized by a relatively sparse supply of GAD/GABA-immunoreactive puncta (e.g., Helfert et al., '89; Roberts and Ribak, '87; this study). The functional role and origin of this innervation is largely unknown, but for the MNTB of the cat, a modulatory role of GABA-ergic input possibly arising in periolivary nuclei has been proposed (Adams and Mugnaini, '90): GABA-mediated inhibition at the level of the MNTB-neuron will lead to disinhibition at the target sites. In the LSO of both bats subregional differences in density of GAD/GABA-positive puncta were noted, but the distributions differ with respect to the tonotopic organizations. In *Rhinolophus*, the highest density occurs in lateral regions where the frequency range below the second harmonic call component is represented. In *Pteronotus*, however, parts of those regions responsive to the second harmonic call component, and especially higher frequencies receive a remarkably dense puncta supply.

The mammalian MSO is generally described as a binaural integration center devoted to processing interaural time and phase differences (review: Irvine, '86). Recent studies of the MSO in bats revealed profound anatomical and functional differences from the classical picture such as a predominance of inputs from the contralateral ear, as well as considerable interspecies variability (Casseday et al., '88; Covey et al., '91; Grothe et al., '92). This suggested a high phylogenetic plasticity at this level of integration.

The GAD- and GABA-staining of the MSO appears to vary across species. In the MSO of gerbils and rats, no positive immunoreactive cells were noted with GAD-antibodies (Roberts and Ribak, '87; Moore and Moore, '87), but in the guinea pig a small subpopulation of cells in the MSO was stained with GABA-antibodies (Peyret et al., '86; Helfert et al., '89). In the MSO of *Pteronotus*, moderately stained somata were observed with GAD- as well as GABA-antibodies, thus excluding the possibility that the presence or absence of labeled cells is due to the use of different antibodies. The morphology of these cells resembled the output neurons projecting to the IC (Zook and Casseday, '82b). The VMSO of *Rhinolophus* contained numerous moderately immunopositive cells, but few cells were labeled in the DMSO.

Although GAD/GABA-immunostaining of cells in MSO varies across species, a common feature is the paucity of GAD/GABA-immunostained puncta. This suggests that GABA-mediated inhibition plays a minor role at this level

Pteronotus

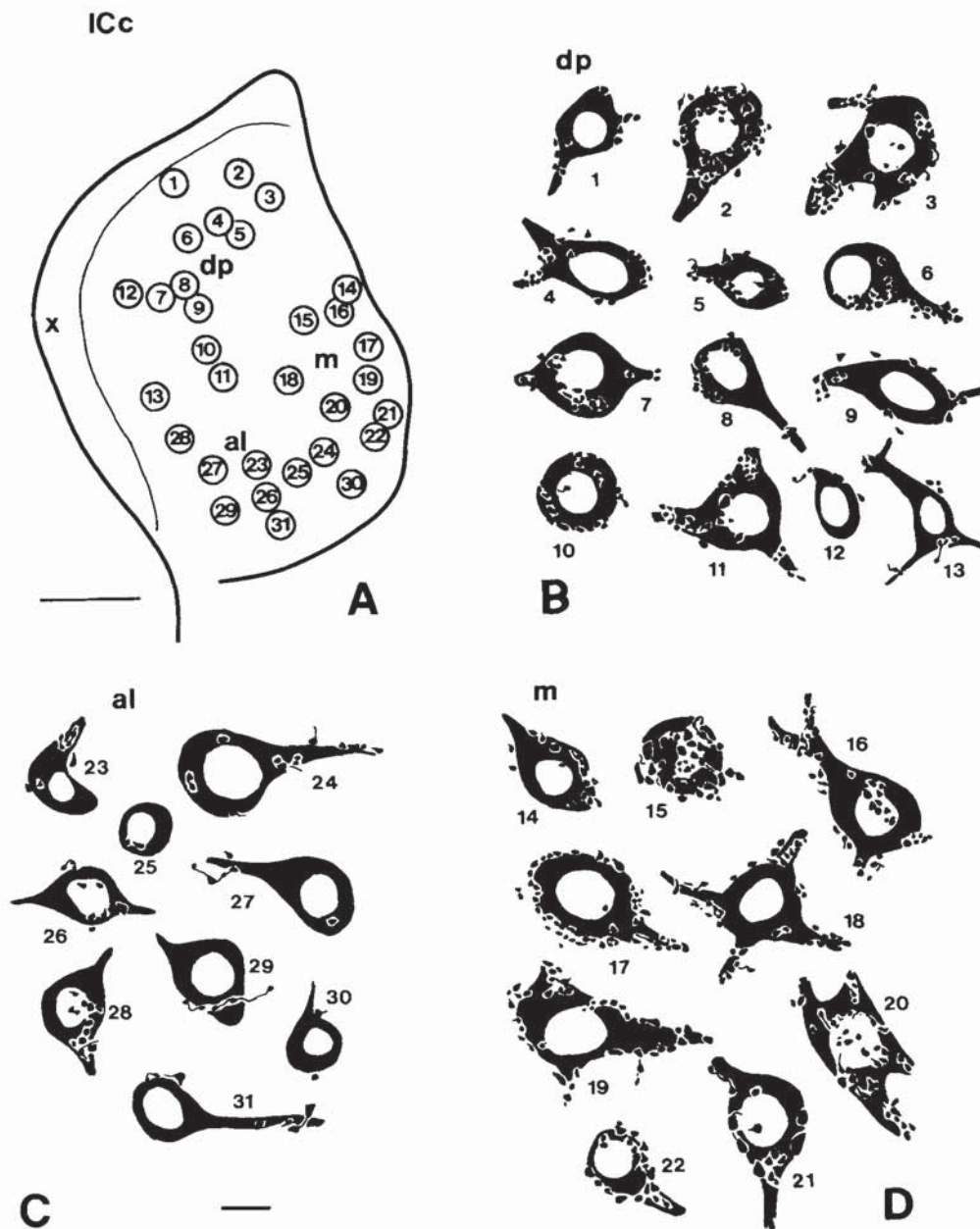


Fig. 13. Drawings of GAD-immunostained cell bodies and their puncta supply in different regions of the ICc of *Pteronotus*. **A:** Survey drawing of the locations of labeled cells in the ICc. Numbers refer to the location of the respective cells within the ICc. **B:** Cell types in the

dorsoposterior division (dp). **C:** Cell types in the anterolateral division (al). **D:** Cell types in the medial division (m). Calibration bars: A = 200 μ m; B–D = 10 μ m.

(e.g., Helfert et al., '89; Adams and Mugnaini, '90; this study). On the other hand, abundant puncta staining was obtained with glycine-antibodies in the MSO of the guinea pig (Helfert et al., '89) and the cat (Adams and Mugnaini, '90), in the MSO of *Pteronotus* and the DMSO and VMSO of *Rhinolophus* (Vater, unpublished). This input is most likely derived from the MNTB (Casseday et al., '88; Adams and Mugnaini, '90; Covey et al., '91). In the mustached bat, glycine has been shown to shape the temporal response

patterns of MSO-cells (Grothe et al., '92). With respect to the status of the medial olivary nuclei of *Rhinolophus*, it is of interest that the GAD/GABA-staining in the VMSO resembles the situation in the MSO of *Pteronotus* more closely than the pattern observed for the DMSO.

In periolivary structures, including those giving rise to the lateral and medial olivocochlear system, the GAD/GABA punctiform labeling is commonly more prominent than in the main nuclei of the SOC and GAD/GABA-

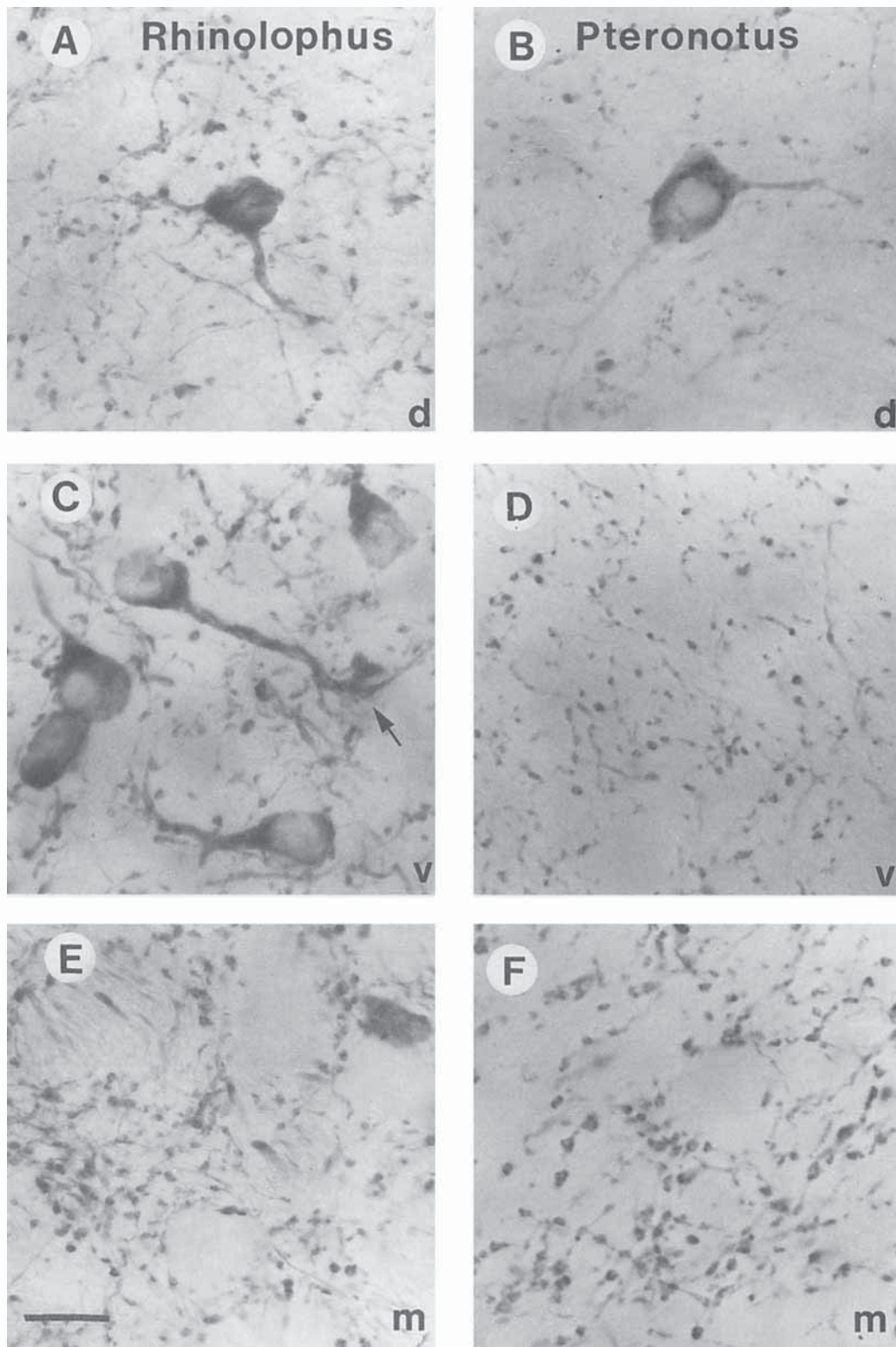


Fig. 14. High power photomicrographs of the GAD-immunostain in the medial geniculate body (MGB) of *Rhinolophus* (left: A, C, E) and *Pteronotus* (right: B, D, F). A: GAD-immunoreactive cell and puncta in the dorsal MGB of *Rhinolophus*. Puncta are located on the soma and along the dendrites of the immunopositive cell. Labeling in the neuropil consists of fibers with fine and coarse varicosities. B: GAD-immunoreactive cell and puncta in the dorsal MGB of *Pteronotus*. Few puncta are observed on the cell body. Labeling in the neuropil consists of scattered puncta and fibers with fine varicosities. C: GAD-immunoreactive cells in the ventral MGB of *Rhinolophus*; dendritic appendages (arrow) of an immunostained cell are surrounding a non-reactive cell. Numerous

puncta of different size and shape are located in the neuropil and on somata and dendrites of immunopositive cells. D: Only GAD-immunostained puncta are observed in the ventral MGB of *Pteronotus*. These encircle the somata of non-stained neurons. E: GAD-immunostained puncta and small cell in the medial MGB of *Rhinolophus*. Puncta of different calibers encircle the somata of non-stained cells and form nests in the neuropil. F: GAD-immunostained puncta ring the somata of non-stained cells in the medial MGB of *Pteronotus*. Many of these puncta are of coarser caliber than those in the ventral and dorsal MGB. Calibration bars: A-F = 10 μ m.

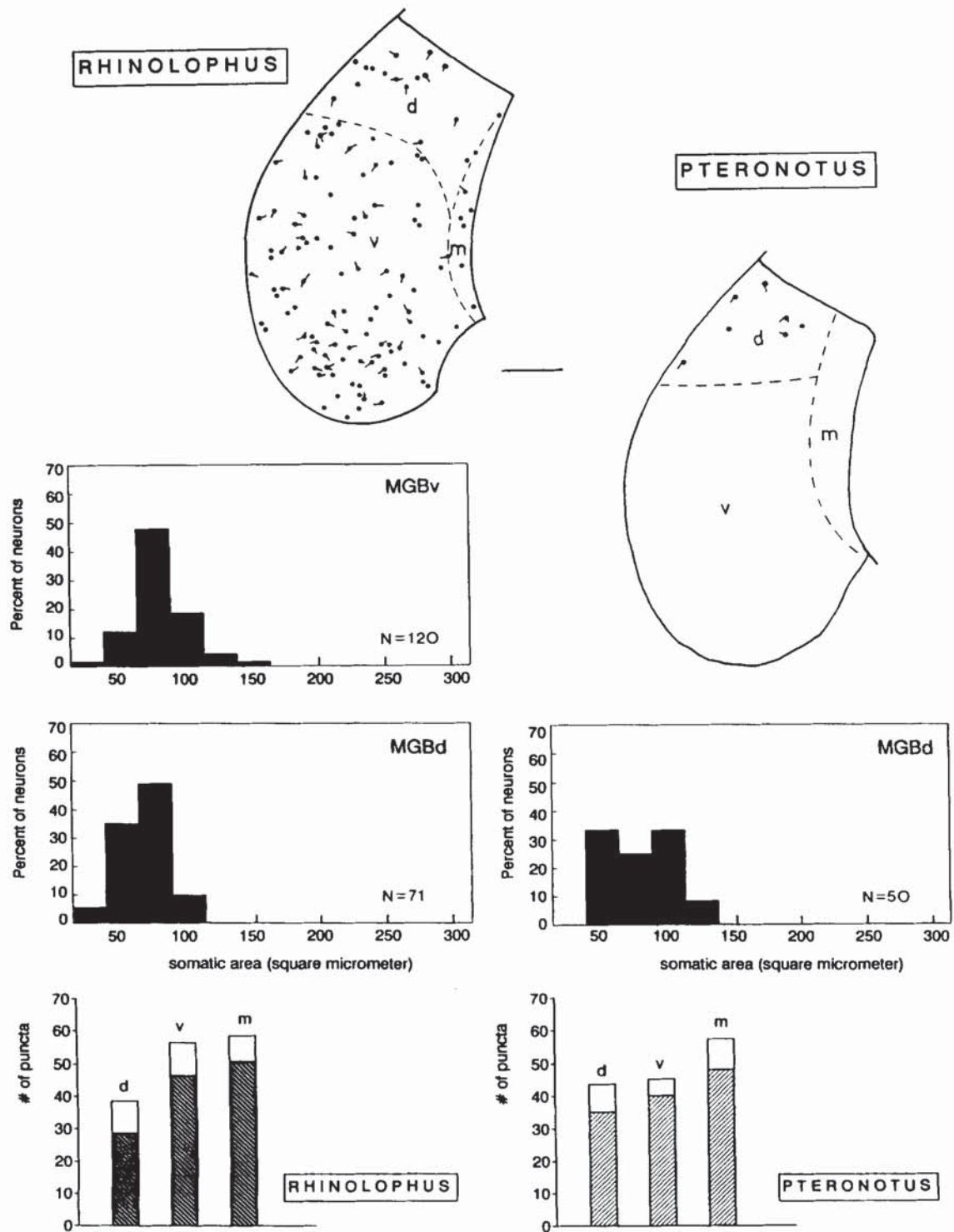


Fig. 15. Schematic illustrations of the distribution of GAD/GABA-immunostained cells (circles) in the medial geniculate body (MGB) of *Rhinolophus* (left) and *Pteronotus* (right). Calibration bar: 200 μm . The orientation of dendrites of immunostained cells is indicated by lines. In *Rhinolophus*, GAD/GABA-immunostained cells are found in all subdivi-

visions of MGB, whereas in *Pteronotus*, they are confined to the dorsal MGB. Bar diagrams give the size of immunostained cells (black bars) and number of puncta per 1,000 μm^2 (obliquely shaded bars) for the different subdivisions of the MGB for both species.

immunoreactive cells are present (e.g., Helfert et al., '89; this study). The olivocochlear system of horseshoe bats differs from that in other species including the mustached bat, since only the lateral component is present, which forms synapses with the afferent endings contacting inner hair cells (e.g., Aschoff and Ostwald, '87). We noted that GAD/GABA-immunoreactive cells were more common in the nucleus of origin of the lateral olivocochlear system in the horseshoe bat than in the mustached bat, but a quantification of this observation is not possible on the present data base. This finding might indicate a difference in the relative importance of GABA-mediated inhibition at the level of the inner hair cell and clearly deserves immunocytochemical studies of the cochlea.

Lateral lemniscus

In bats, as in all species studied so far, the DNLL contains the highest population density of putatively GABAergic cells in the auditory system (Adams and Mugnaini, '84; Peyret et al., '86; Roberts and Ribak, '87). Most, if not all, of them are projection neurons which provide input to the ipsilateral and contralateral IC (Adams and Mugnaini, '84; Shneiderman et al., '88). DNLL-cells also receive a dense supply of immunoreactive puncta. According to tracer studies (Shneiderman et al., '88), one major source of putatively GABAergic input might be the reciprocal connection between the DNLLs of both sides.

Consequently, the DNLL in all mammals studied so far is a major source of feedforward inhibition at the midbrain level and its action in turn can be influenced by inhibitory inputs. It is especially interesting that in *Rhinolophus*, the PLZ also stains prominently for GABAergic-markers. Cells in the PLZ are excited by acoustic stimuli and their responses are distinctly influenced by motor commands during active vocalization (Metzner, '89). Consequently, the PLZ represents an auditory-vocal interface. The large number of GAD/GABA-positive cells suggests that it acts as an inhibitory relay within the vocalization pathway. Such a function is consistent with requirements for regulatory control of discharge rate in the nucleus ambiguus during active Doppler-shift compensation (Metzner, '89). It is further noteworthy that cells of the PLZ receive distinct input from GAD/GABA-positive puncta; this argues for the presence of inhibitory pathways for fine control of neuronal activity. According to tracer studies (Metzner, '89) one possible source of such input is the contralateral PLZ. In the mustached bat, which also actively compensates for Doppler-shifts during echolocation (review: Schnitzler and Henson, '80), we could not clearly define a separate PLZ. However, immunostained cell types in medial DNLL and at its rostral pole are similar to those in the PLZ of *Rhinolophus*. Whether they serve a similar function needs to be tested in recordings during active vocalization and by analysis of projection patterns.

The INLL and VNLL of bats exhibited a regional specific pattern of immunostaining for GABAergic markers, which contrasts with the quite uniform distribution pattern observed in rats (Moore and Moore, '87). In the INLL, the pattern corresponds partially to the tonotopic organization. In *Pteronotus*, the laterodorsal part, responsive to the second harmonic CF-component of the orientation call (Ross et al., '88), contains the highest density of puncta; similarly, immunostain is heaviest in medial regions of the INLL of *Rhinolophus*, representing the second harmonic CF-component (Metzner and Radtke-Schuller, '87). In the

VNLL, the immunostain correlates with distinct cytoarchitectonic subdivisions. In both species, the areas receiving input from large calyces supplied by axons of CN cells (i.e., the medial region in *Rhinolophus* (Vater and Feng, '90) and the ventral region in *Pteronotus* (Zook and Casseday, '85)) lack distinct GAD/GABA-immunoreactive somata and only receive sparse puncta in comparison with other VNLL-subregions. Cells in VNLLm of horseshoe bats are darkly stained with glycine antibodies and presumably act as relays in a fast ascending pathway from the CN, mediating inhibition at the midbrain level (Vater et al., '92).

Inferior colliculus

The general pattern of GAD/GABA-staining in the IC of bats conforms to data from other mammals (Thompson et al., '85; Roberts and Ribak, '87; Moore and Moore, '87; Caspary et al., '90). Different types of labeled cells within the ICc were noted in all species, but a newly described feature is the remarkable regional variation in puncta density across the ICc. This variation indicates regional differences in inhibitory input and needs to be discussed in relation to the tonotopic organization and in the context of segregations of parallel ascending pathways from the lower brainstem within isofrequency planes. The abundance of GAD/GABA-stained somata and puncta is consistent with the fact that the response properties of IC-neurons reflect prominent inhibitory input. Ionophoretic studies of the ICc in rats (e.g. Faingold et al., '89), horseshoe bats (Vater et al., '92) and mustached bats (e.g., Pollak and Park, '92) have demonstrated that GABAergic mechanisms are involved in both monaural and binaural signal processing.

Similar to other mammals (e.g., Moore and Moore, '87; Caspary et al., '90), a large heterogenous population of GAD/GABA-immunoreactive somata is observed throughout the ICc of both bats. The exact cell types can not be identified in our material; however, the criteria of soma size and the orientation of dendritic trunks could suggest that GAD/GABA-immunopositive cells belong to different classes of disc-shaped cells and stellate cells identified in Golgi-material (Oliver and Morest, '84; Zook et al., '85). Since it was shown that most neurons in the IC give off collaterals within the colliculus (review: Oliver and Shneiderman, '91), GAD/GABA-immunostained IC-cells may well contribute to local interactions within and across fibrodendritic laminae in addition to participation in efferent projections. These suggestions are necessarily speculative, given the absence of combined tracing and immunocytochemical data. A partial regional segregation of GAD/GABA-immunopositive cell types within the ICc is indicated by the following observations. In the ICc of horseshoe bats, the population of immunopositive cells in the ventral aspect of the ICc is clearly different from that in other subregions, since it comprises mainly intermediate sized cells, which receive only very few immunopositive puncta. These ventral regions are probably not separate tonotopic zones. According to anterograde transport patterns of horseradish peroxidase (e.g., Casseday et al., '88; Vater and Feng, '90) and neurophysiological evidence (Rübsamen and Schäfer, '90), they may represent the ventral continuation of isofrequency laminae, which exhibit an onion-skin organization throughout the ICc. The functional significance of this finding deserves further study but may be indicative of differences in organization within an isofrequency lamina. In *Pteronotus*, ventral regions of the ICc are also characterized by low density of GAD/GABA-immunopositive puncta

and a predominance of smaller GAD/GABA-immunopositive cells. These regions seem to encompass all three ICc-subdivisions, but their exact relation to the specialized course of isofrequency laminae in this species (Zook et al., '85) remains to be determined. In both bats, the ICc is characterized by prominent regional differences in the amount of putatively GABAergic inhibitory input, most clearly evidenced by the presence of a band of low puncta density in lateral aspects of the ICc. In *Rhinolophus*, the location and orientation of this band partially encompasses the representation places of cells tuned to frequencies below the CF-component. A functional characterization of this ICc-region and information on its full contingent of inputs remains to be obtained. It is noteworthy that this region is characterized by a high density of glycine-immunopositive puncta (Vater et al., '90) indicating a partial segregation of neurochemical bands within the ICc. In *Pteronotus*, a band of low density of GAD/GABA-immunopositive puncta is found in lateral aspects of the dorsoposterior division. According to Ross et al. ('88), these zones receive predominant inputs from the VNLL and the MSO.

In addition to intrinsic connections, possible sources of putatively GABAergic inhibitory input to the ICc are the subpopulations of immunopositive cells within the INLL, VNLL, the principal nuclei of the SOC, the periolivary nuclei, and the contralateral ICc. If and how these cells contribute to the GAD/GABA-immunolabeling of puncta in the ICc remains to be determined. The major lower brainstem source of GABAergic inhibitory input to the colliculus is the DNLL, which projects bilaterally to the ICc (horseshoe bat: Schweizer, '81; Metzner, '89; mustached bat: e.g., Zook and Casseday, '87). In neither bat species does the banding pattern of this input fully reflect the distribution of GAD/GABA-immunopositive puncta in the ICc: DNLL-inputs appear to be largely confined to the ventral two thirds of the ICc-volume. Consequently, GAD/GABA-immunopositive puncta found in dorsal aspects of the ICc are expected to be derived from other sources. This observations could indicate a segregation of putatively GABAergic input derived from different sources along the extent of isofrequency planes and clearly needs to be further studied in combined tracing and immunocytochemical studies.

Medial geniculate body

GAD/GABA-immunoreactive somata are found in all subdivisions of the MGB in rodents (Ottersen and Storm-Mathisen, '84; Winer and Larue, '88) and the cat (Rouiller et al., '90). In bats, the GAD/GABA-immunostaining in the MGB reveals a prominent species specific difference. In the horseshoe bat, the ventral and medial MGB contain subpopulations of GAD/GABA-positive neurons which are lacking in the mustached bat (see also Winer and Wenstrup, '87). On the other hand the dorsal MGB of both species contains GAD/GABA-positive cells. Data in other mammals show that the connectivity and consequently the function of the MGB-subdivisions differ (e.g., Winer et al., '77). Specifically, the ventral MGB is the main acoustic relay center to the primary auditory cortex, whereas the medial MGB is a multimodal relay center and projects to all regions of the auditory cortex in the cat (Winer et al., '77; Winer and Morest, '83). The dorsal MGB is mainly auditory, but also receives somatic inputs and projects to all cortical auditory areas with the exception of AI (Winer et al., '77). The GAD/GABA-positive cell types in the ventral MGB of *Rhinolophus* and in particular their dendritic morphology

closely resemble those found in the rat (Winer and Larue, '88). They thus possibly correspond to Golgi II cells, which represent local inhibitory neurons in other species. In particular, the observation that as in the rat (Winer and Larue, '88), the dendrites of GAD/GABA-positive cells can be in close apposition to neighboring cells could indicate the presence of local circuits with putatively inhibitory function in the fine control of neuronal activity. This suggestion needs, however, to be supported by immuno-electron microscopy. It is unknown in the horseshoe bat where the axons of GAD/GABA-positive cells of the MGB terminate, i.e., whether they are intrinsic inhibitory interneurons, or project to more distant targets. The striking species difference between the horseshoe bat and the mustached bat is of potential functional significance, since it indicates the presence of a prominent substrate for inhibitory interactions in the MGB of *Rhinolophus*, either involving local circuits or projections to the cortex. The absence of such a network in the ventral and medial MGB of *Pteronotus*, should be reflected in physiological response characteristics within the MGB itself (e.g., levels of spontaneous activity and complexity of response patterns, see Rouiller et al., '90) as well as in the target projection zones, but so far physiological evidence is lacking. It is surprising that such a prominent difference appears to exist in two species within the same mammalian order. Given the fact that the two non-related bats have developed almost identical echolocation systems in convergent evolution, a functional explanation cannot be straightforward, but will require detailed physiological studies as well as comparative analyses of the connectivity.

Some trends observed in the gross pattern of puncta labeling in the MGB of both bats appeared similar and compatible with other species. Similar to the rat (Winer and Larue, '88), puncta tended to be coarser in medial parts of the MGB than in other subdivisions. A tendency for a less abundant staining of puncta in the dorsal MGB as compared to other regions was present, although less pronounced than in the rat. Within gross subdivisions of the MGB of both bats, subregional variations in puncta pattern were noted. These clearly deserve further analysis but a more detailed interspecies comparison has to wait until more data on the functional organization of the MGB of bats are available.

ACKNOWLEDGMENTS

We are especially grateful to Dr. Wolfgang Oertel for kindly supplying the GAD-antibody. We thank Drs. Jean Büttner-Ennever, Gerhard Neuweiler, and George Pollak for helpful discussions and critical comments on several versions of the manuscript; Dr. Jenny Kien for corrections of the final version; and Hildegard Hallmer and Ruth Novak for photographic work. This research was supported by the SFB 204 and SFB 220.

LITERATURE CITED

- Adams, J.C., and E. Mugnaini (1984) Dorsal nucleus of the lateral lemniscus: A nucleus of GABAergic projection neurons. *Brain Res. Bull.* 13:585-590.
- Adams, J.C., and E. Mugnaini (1987) Patterns of glutamate decarboxylase immunostaining in the feline cochlear nuclear complex studied with silver enhancement and electron microscopy. *J. Comp. Neurol.* 286:375-401.
- Adams, J.C., and E. Mugnaini (1990) Immunocytochemical evidence for inhibitory and disinhibitory circuits in the superior olive. *Hear. Res.* 49:281-298.

- Aschoff, A., and J. Ostwald (1987) Different origins of cochlear efferents in some bat species, rats and guinea pigs. *J. Comp. Neurol.* 264:56-73.
- Bishop, A.L., and O.W. Henson, Jr. (1987) The efferent cochlear projections of the superior olivary complex in the mustached bat. *Hear. Res.* 31:175-182.
- Caspary, D.M. (1986) Cochlear nuclei: Functional neuropharmacology of the principal cell types. In R.A. Altschuler, D.W. Hoffmann, and R.P. Bobbin (eds): *Neurobiology of Hearing: The Cochlea*. New York: Raven Press, pp. 303-332.
- Caspary, D.M., D.C. Havey, and C.L. Faingold (1979) Effects of microiontophoretically applied glycine and GABA on neuronal response patterns in the cochlear nuclei. *Brain Res.* 172:179-185.
- Caspary, D.M., A. Raza, B.A. Lawhorn Armour, J. Pippin, and S.P. Arneric (1990) Immunocytochemical and neurochemical evidence for age-related loss of GABA in the inferior colliculus: Implications for neural presbycusis. *J. Neurosci.* 10:2363-2372.
- Casseday, J.H., E. Covey, and M. Vater (1988) Connections of the superior olivary complex in the rufous horseshoe bat, *Rhinolophus rouxi*. *J. Comp. Neurol.* 278:313-330.
- Covey, E., M. Vater, and J.H. Casseday (1991) Binaural properties of single units in the superior olivary complex of the mustached bat. *J. Neurophysiol.* 66:1080-1095.
- Faingold, C.L., G. Gehlbach, and D.M. Caspary (1989) On the role of GABA as an inhibitory neurotransmitter in inferior colliculus neurons: Ionophoretic studies. *Brain Res.* 500:302-312.
- Feng, A.S., and M. Vater (1985) Functional organization of the cochlear nucleus of rufous horseshoe bats (*Rhinolophus rouxi*): Frequencies and internal connections are arranged in slabs. *J. Comp. Neurol.* 235:529-553.
- Grothe, B., M. Vater, J.H. Casseday, and E. Covey (1992) Monaural interaction of excitation and inhibition in the medial superior olive of the mustached bat: An adaptation for biosonar. *Proc. Natl. Acad. Sci.* 89:5108-5112.
- Helfert, R.H., J.M. Bonneau, R.J. Wenthold, and R.A. Altschuler (1989) GABA and glycine immunoreactivity in the guinea pig superior olivary complex. *Brain Res.* 501:269-286.
- Hsu, S.M., L. Raine, and H. Fanger (1981) Use of Avidin-Biotin-Peroxidase complex (ABC) in immunoperoxidase techniques. *J. Histochem. Cytochem.* 29:577-580.
- Irvine, D.R.F. (1986) *The Auditory Brainstem*. Progress in Sensory Physiology 7. Berlin—Heidelberg—New York: Springer Verlag.
- Kössl, M., and M. Vater (1990) Tonotopic organization of the cochlear nucleus of the mustache bat, *Pteronotus parnellii*. *J. Comp. Physiol. A* 166:695-709.
- Kössl, M., M. Vater, and H. Schweizer (1988) Distribution of catecholamine fibers in the cochlear nucleus of horseshoe bats and mustache bats. *J. Comp. Neurol.* 269:523-534.
- Metzner, W. (1989) A possible neuronal basis for Doppler-shift compensation in echolocating horseshoe bats. *Nature* 341:529-532.
- Metzner, W., and S. Radtke-Schuller (1987) The nuclei of the lateral lemniscus in the rufous horseshoe bat, *Rhinolophus rouxi*. *J. Comp. Neurol.* 260:395-411.
- Möller, J. (1978) Response characteristics of inferior colliculus neurons of the awake CF-FM bat *Rhinolophus ferrumequinum*. II. Two-tone stimulation. *J. Comp. Physiol.* 125:227-236.
- Moore, J.K., and R.Y. Moore (1987) Glutamic acid decarboxylase-like immunoreactivity in brainstem auditory nuclei of the rat. *J. Comp. Neurol.* 260:157-174.
- Müller, C.M., and H. Scheich (1987) GABAergic inhibition increases the neuronal selectivity to natural sounds in the avian auditory forebrain. *Brain Res.* 414:376-380.
- Mugnaini, E. (1985) GABA neurons in the superficial layers of the rat dorsal cochlear nucleus: Light and electron microscopic immunocytochemistry. *J. Comp. Neurol.* 235:61-81.
- Neuweiler, G., and M. Vater (1977) Response patterns to pure tones of cochlear nucleus units in the CF-FM bat, *Rhinolophus ferrumequinum*. *J. Comp. Physiol.* 115:119-133.
- Oertel, W.H., D.E. Schmechel, E. Mugnaini, M.L. Tappaz, and I.J. Kopin (1981) Immunocytochemical localization of glutamate decarboxylase in rat cerebellum with a new antiserum. *Neurosci.* 6:2715-2735.
- Oliver, D.L., and D.K. Morest (1984) The central nucleus of the inferior colliculus in the cat. *J. Comp. Neurol.* 222:237-264.
- Oliver, D.L., and A. Shneiderman (1991) The anatomy of the inferior colliculus: A cellular basis for integration of monaural and binaural information. In R.A. Altschuler et al. (eds): *Neurobiology of Hearing: The Central Auditory System*. New York: Raven Press Ltd, pp. 195-222.
- Osen, K.K., and E. Mugnaini (1981) Neuronal circuits in the dorsal cochlear nucleus. In J. Syka and L. Aitkin (eds): *Neuronal Mechanisms of Hearing*. New York—London: Plenum Press, pp. 119-125.
- Ottersen, O.P., and J. Storm-Mathisen (1984) GABA-containing neurons in the thalamus and pretectum of the rodent. *Anat. Embryol.* 170:197-207.
- Peyret, D., M. Geffard, and J.M. Aran (1986) GABA immunoreactivity in the primary nuclei of the auditory central nervous system. *Hear. Res.* 23:115-121.
- Pollak, G.D., and J.H. Casseday (1989) *The Neural Basis of Echolocation in Bats*. Berlin: Springer-Verlag.
- Pollak and Park (1992) The role of GABA in shaping monaural response properties of neurons in the inferior colliculus. Abstracts 18th Midwinter meeting ARO, p. 236.
- Roberts, R.C., and C.E. Ribak (1987) GABAergic neurons and axon terminals in the brainstem auditory nuclei of the gerbil. *J. Comp. Neurol.* 258:267-280.
- Rouiller, R.M., M. Capt, J.P. Hornung, and P. Streit (1990) Correlation between regional changes in the distributions of GABA-containing neurons and unit response properties in the medial geniculate body of the cat. *Hear. Res.* 49:249-258.
- Ross, L.S., G.D. Pollak, and J.M. Zook (1988) Origin of ascending projections to an isofrequency region of the mustache bat's inferior colliculus. *J. Comp. Neurol.* 270:488-505.
- Rübsamen, R., and M. Schäfer (1990) Ontogenesis of auditory fovea representation in the inferior colliculus of the Sri lanka rufous horseshoe bat, *Rhinolophus rouxi*. *J. Comp. Physiol.* 167:757-770.
- Saint Marie, R.L., D.K. Morest, and C.J. Brandon (1989a) The form and distribution of GABAergic synapses on the principal cell types of the ventral cochlear nucleus of the cat. *Hear. Res.* 42:97-112.
- Saint Marie, R.L., E.M. Ostapoff, D.K. Morest, and R.J. Wenthold (1989b) Glycine-immunopositive projection of the cat lateral superior olive: Possible role in midbrain ear dominance. *J. Comp. Neurol.* 279:382-396.
- Saint Marie, R.L., C.G. Benson, E.-M. Ostapoff, and D.K. Morest (1991) Glycine immunoreactive projections from the dorsal to the anteroventral cochlear nucleus. *Hear. Res.* 51:11-28.
- Schlegel, P. (1977) Directional coding by binaural brainstem units of the CF-FM bat, *Rhinolophus ferrumequinum*. *J. Comp. Physiol.* 118:327-352.
- Schnitzler, H.-U., and O.W. Henson, Jr. (1980) Performance of airborne animal sonar systems: I. Microchiroptera. In R.G. Busnel and J.F. Fish (eds): *Animal Sonar Systems*. New York: Plenum Press, pp. 109-181.
- Schweizer, H. (1981) The connections of the inferior colliculus and the organization of the brainstem auditory system in the Greater horseshoe bat (*Rhinolophus ferrumequinum*). *J. Comp. Neurol.* 270:25-49.
- Shneiderman, A., D.L. Oliver, and C.K. Henkel (1988) Connections of the dorsal nucleus of the lateral lemniscus: An inhibitory parallel pathway in the ascending auditory system? *J. Comp. Neurol.* 276:188-208.
- Spangler, K.M., N.B. Cant, C.K. Henkel, G.R. Farley, and W.B. Warr (1987) Descending projections from the superior olivary complex to the cochlear nucleus of the cat. *J. Comp. Neurol.* 259:452-465.
- Sternberger, L.A. (1979) *Immunocytochemistry*, 2nd edn. New York: John Wiley & Sons, p. 354.
- Thompson, G.C., A.M. Cortez, and D. Man-Kit Lam (1985) Localization of GABA immunoreactivity in the auditory brainstem of guinea pigs. *Brain Res.* 339:119-122.
- Vater, M., and A.S. Feng (1990) The functional organization of ascending and descending connections of the cochlear nucleus of horseshoe bats. *J. Comp. Neurol.* 292:373-395.
- Vater, M., M. Kössl, and A.K.E. Horn (1990) Differential distribution of GABA and glycine in the ascending auditory pathway of horseshoe bats. In N. Elsner and G. Roth (eds): *Brain—Perception—Cognition. Proceedings of the 18th Göttinger Neurobiologentagung*. Stuttgart—New York: Georg Thieme Verlag, p. 142.
- Vater, M., H. Habbicht, M. Kössl, and B. Grothe (1992) The functional role of GABA and glycine in monaural and binaural signal analysis in the inferior colliculus of horseshoe bats. *J. Comp. Physiol.* (in press).
- Vater, M., M. Kössl, and A.K.E. Horn (1992) Immunocytochemical aspects of the functional organization of the horseshoe bat's cochlear nucleus. In W.A. Ainsworth, E.F. Evans and C.M. Hackney (eds): *Cochlear Nucleus: Structure and Function in Relation to Modelling*. Vol. III of *Advances in Speech, Hearing and Language Processing*. London: JAI Press LTD., in press.
- Wenstrup, J.J., L.S. Ross, and G.D. Pollak (1986) Binaural response organization within a frequency band representation of the inferior colliculus: Implications for sound localization. *J. Neurosci.* 6:962-973.

- Wentholt, R.J., J.M. Zempel, M.H. Parakkal, K.A. Reeks, and R.A. Altschuler (1986): Immunocytochemical localization of GABA in the cochlear nucleus of the guinea pig. *Brain Res.* 380:7-18.
- Wentholt, R.J., D. Huie, R.A. Altschuler, and K.A. Reeks (1987) Glycine immunoreactivity localized in the cochlear nucleus and superior olivary complex. *Neuroscience* 22:897-912.
- Wickesberg, R.E., and D. Oertel (1988) Tonotopic projection from the dorsal to the anteroventral cochlear nucleus of mice. *J. Comp. Neurol.* 268:389-399.
- Winer, J.A., and D.K. Morest (1983) The medial division of the medial geniculate body of the cat: Implications for thalamic organization. *J. Neurosci.* 12:2629-2651.
- Winer, J.A., and D.T. Larue (1988) Anatomy of glutamic acid decarboxylase immunoreactive neurons and axons in the rat medial geniculate body. *J. Comp. Neurol.* 278:47-68.
- Winer, J.A., and J.J. Wenstrup (1987) Anatomy of the mustache bat's medial geniculate body: Cytoarchitectonics, neuronal architecture, and GAD-immunoreactivity. *Proc. Soc. Neurosci.* 13:324.
- Winer, J.A., I.T. Diamond, and D. Raczkowski (1977) Subdivisions of the auditory cortex of the cat: The retrograde transport of horseradish peroxidase to the medial geniculate body and posterior thalamic nuclei. *J. Comp. Neurol.* 176:387-418.
- Winter, I.M., D. Robertson, and K.S. Cole (1989) Descending projections from auditory brainstem nuclei to the cochlea and cochlear nucleus of the guinea pig. *J. Comp. Neurol.* 280:143-157.
- Zook, J.M., and J.H. Casseday (1982a) Cytoarchitecture of the auditory system in the lower brainstem of the mustache bat, *Pteronotus parnellii*. *J. Comp. Neurol.* 207:1-13.
- Zook, J.M., and J.H. Casseday (1982b) Origin of ascending projections to the inferior colliculus in the mustache bat, *Pteronotus parnellii*. *J. Comp. Neurol.* 207:14-28.
- Zook, J.M., and J.H. Casseday (1985) Projections from the cochlear nuclei in the mustache bat, *Pteronotus parnellii*. *J. Comp. Neurol.* 237:307-324.
- Zook, J.M., and J.H. Casseday (1987) Convergence of ascending pathways at the inferior colliculus of the mustache bat, *Pteronotus parnellii*. *J. Comp. Neurol.* 261:347-361.
- Zook, J.M., J.A. Winer, G.D. Pollak, and R.D. Bodenhamer (1985) Topology of the central nucleus of the mustache bat's inferior colliculus: Correlation of single unit properties and neuronal architecture. *J. Comp. Neurol.* 231:530-547.